

**PROTON  
THERAPY  
C O -  
OPERATIVE  
GROUP**

Chair  
Michael Goitein Ph. D  
Department of Radiation Oncology  
Massachusetts General Hospital  
Boston MA 02114  
(617) 724 - 9529  
(617) 724 - 9532 Fax  
Goitein@hadron.mgh.harvard.edu

Secretary  
Janet Sisterson Ph. D.  
Northeast Proton Therapy Center  
Massachusetts General Hospital  
30 Fruit Street  
Boston MA 02114  
(617) 724 - 1942  
(617) 724 - 9532 Fax  
Sisterson@radonc.mgh.harvard.edu

**ABSTRACTS**  
  
**of the**  
**XXX PTCOG MEETING**

**held in**  
**Cape Town, South Africa**

**April 12 - 15 1999**

## INDEX

Page

### Beam Scanning Workshop

Development of a scanning system for proton therapy in Uppsala. 5  
*S. Lorin, N. Tilly, J. Medin, M. Blom, V. Ziemann, B. Glimelius and E. Grusell*

Experience of 3-D proton beam spot scanning at NIRS. 6  
*K. Kawachi and T. Kanai*

### Neutrons: Physical Aspects (ECHED Mini Symposium)

Quality control of neutron beam: a cooperative study of ECHED. 6  
*N. Iborra-Brassart*

Design considerations for a computer controlled multileaf collimator 7  
for the Harper Hospital fast neutron therapy facility.  
*R. L. Maughan, M. Yudelev, J. D. Forman, E. B. Blosser, S. B. Williams, D. Gries,  
W. Chapman, and T. M. Fletcher*

Program for the optimization of multiblade trimmer blade positions. 7  
*C. van Gend, E. A. de Kock, and A. N. Schreuder*

Microdosimetric response of carbon and oxygen in a p(66)/Be(40) THERAPY beam. 8  
*P. J. Binns and A. N. Schreuder*

### Boron Neutron Capture Therapy (ECHED Mini Symposium)

Progress report on the BNC enhancement studies at the Seattle fast neutron therapy beam 8  
and other developments.  
*R. Risler, G. E. Laramorer, K. S. Stelzer, D. W. Nigg, C. A. Wemple, J. K. Hartwell and Y. D. Harker*

Dosimetry studies for boron neutron capture therapy and the feasibility of boron neutron capture 9  
enhanced fast neutron therapy at the Gershenson Radiation Oncology Center.  
*R. L. Maughan, C. Kota, J. W. Burmeister and J. D. Forman*

TLD-600 and TLD-700: a possible way to measure the thermal component in a fast neutron beam. 9  
*N. Iborra-Brassart, J. P. Pignol, J. Hérault, and P. Chauvel*

### Radiobiology

Reliability of the micronucleus assay for predicting radiosensitivity. 10  
*J. M. Akudugu, J. P. Slabbert, A. Serafin, and L. Bohm*

Comparison between dna and cytogenetic damages in lymphocytes from healthy donors 11  
and skin cancer patients.  
*A. Cebulska-Wasilewska, W. Dyga, S. Krasnowolski, A. Wierzevska, and E. Budzanowska*

Proton irradiation and dose-volume effects in the rat spinal cord. 12  
*H.P. Bijl, A.J. van der Kogel, P. van Luijk, J.M. Schippers, R. Coppes, B.G. Szabó and A.W.T. Konings*

## Eye Treatments

Treatment planning of eye tumors: problems encountered. <i>N. Iborra-Brassart, J. Herault, P.Y. Bondiau, A. Courdi, and P. Chauvel</i>	13
Uveal melanomas: results of protontherapy in Nice. <i>P. Chauvel, A. Courdi, J.P. Caujolle, J.D. Grange, L. Diallo-Rosier, J. Sahel, F. Bacin, C. Zur, N. Iborra-Brassart, J. Herault, and P. Gastaud</i>	14
Proton Beam Therapy for Age-related Macular Degeneration: Development of a Standard Plan. <i>J. A. Adams, K. L. Paiva, J. E. Munzenrider, J. W. Miller, and E. S. Gragoudas</i>	14
The treatment of age-related macular degeneration using the Clatterbridge proton beam. <i>A. Kacperek, M. C. Briggs, R. D. Errington, S. P. Harding, B. Jones, M. A. Sheen and J. Kongerud</i>	15
Preliminary results of protontherapy in age related macular degeneration. <i>P. Chauvel, C. Zur, J.P. Caujolle, N. Iborra-Brassart, J. Herault, N. Pinto, A. Courdi, and P. Gastaud</i>	16

## Clinical: General

Treatment of tumours of the nose, paranasal sinuses and orbit with neutron and proton therapy. <i>C. Stannard, J. Wilson, A.I O’Ryan, S. Fredericks</i>	17
The potential use of proton therapy in the management of craniopharyngiomas in children. <i>J. L. Habrand, H. Mammar, R. Ferrand, C. Kalifa</i>	17
Proton fractionated stereotactic radiosurgery for secreting pituitary adenoma: the NAC experience. <i>J. K. Harris, F. J. A. Vernimmen, J. Wilson, M. Conradie</i>	18
Dose-volume relationships in radiosurgery. <i>B. J. Smit</i>	18
High dose proton-photon therapy in the management of aggressive intra-cranial malignancies: update of the Orsay series. <i>J. L. Habrand, H. Mammar, N. Gokarn, C. Haie, D. Pontvert, C. Lenir, R. Ferrand, A. Rey, J. J. Mazeron</i>	19

## Facilities and Equipment

The new energy degrading system for the NAC proton therapy beam. <i>A N. Schreuder A. Kiefer, J. van der Merwe, A. Muller, K. Langen, and J. E. Symons</i>	19
CT Scanner for imaging upright patients. <i>A. J. Lennox and T. K. Kroc</i>	20
A design of a compact gantry for proton therapy with 2D-scanning. <i>H. Vrenken, R. Schuitema, O. C. Dermois and J. M. Schippers</i>	20

## Patient Positioning

Organ Motion. <i>K. M. Langen, D.T.L. Jones</i>	21
Improvements to the NAC proton position verification system. <i>C. van Gend, E. A. de Kock, and A. N. Schreuder</i>	21

	<b>Page</b>
Digital x-ray imaging system for patient positioning at CPO. <i>S Delacroix, R Ferrand, C Richaud, and E Brune</i>	22
<b>Dosimetry</b>	
An international code of practice for external beam radiotherapy based on absorbed-dose-to-water standards: proton beams. <i>P. Andreo, D. Burns, K. Hohlfeld, M. S. Huq, T. Kanai, F. Laitano, V. Smyth, and S. Vynckier</i>	22
Clinical use of heavy particle dosimetry with ESR (Electron Spin Resonance Spectroscopy). <i>F.-J. Prott, U. Haverkamp, C. Wiezorek, and M. Hoffmann</i>	23
Water Calorimetry and Ionisation Chamber Dosimetry in Collimated Photon, Proton, and Neutron Beams of Various Energies. <i>H.J. Brede, K.-D. Greif, O. Hecker, P.J. Binns, K. Langen, D.T.L. Jones, A.N. Schreuder, J. Heese and H. Kluge</i>	24
Proton dosimetry intercomparison using parallel plate ion chambers at the PSI-OPTIS proton therapy beam. <i>A. Kacperek, E. Egger, A. Amat, L. Barone Tonghi, G. Cuttone, L. Raffaele, A. Rovelli, P. Tabarelli de Fatis, F. Luraschi, and L. Marzoli</i>	24
Proton dosimetry in small irradiation fields. <i>P. van Luijk and J. M. Schippers</i>	25
Experimental study of perturbation correction factors for ionization chambers in a 75 MeV clinical beam. <i>H. Palmans, S. Vynckier, J.-M. Denis, F. Verhaegen and H. Thierens</i>	26
<b>Planning and beam characterization</b>	
Comparative plans for existing and new proton beamlines at the NAC. <i>A.O’Ryan, N. Schreuder, J. Wilson, C. Stannard, F.Vernimmen, R.Abratt, and B.Smit</i>	27
Case report on a 12-year-old girl with recurrent benign schwannoma treated with proton therapy. <i>D. E. Commin, A. O’Ryan, C. E. Stannard, J. Wilson, F. J. A. Vernimmen, and A. N. Schreuder</i>	27
Test of GEANT/FLUKA with 160 MeV protons stopping in copper. <i>B. Gottschalk, R. Platais, and H. Paganetti</i>	28
Implementing the ISO 90001/QART quality system in proton radiotherapy. <i>A. Kacperek, M. A. Sheen, K. Sztanko, J. Kongerud and B. Marsland</i>	29
<b>Poster Presentations</b>	
Current status of hadron therapy at the South African National Accelerator Centre. <i>D. T. L. Jones, A. N. Schreuder, J. E. Symons, E. A. de Kock, F. J. A. Vernimmen, C. E. Stannard, J. Wilson and J. K. Harris</i>	30
The gamma dose component in a p(66)/Be neutron therapy beam. <i>D. T. L. Jones, A. N. Schreuder and J. E. Symons</i>	30
Pencil beam convolution model for fast dose calculations in uncharged particle radiation treatment planning. <i>E. A. de Kock</i>	31
Energy spectra measured outside the NAC neutron therapy vault. <i>V. M. P. Xulubana and P. J. Binns</i>	31

**Page**

TLD measurements in the hadron therapy beams at NAC. <i>J. Bhengu, P. J. Binns, D. T. L. Jones, K. M. Langen, M. Meincken and J. E. Symons</i>	32
Correcting microdosimetric spectra for pileup. <i>K. Langen, P. Binns, A. Lennox, T. Kroc and P. DeLuca</i>	32
Dedicated Monte Carlo codes for the NAC proton therapy beam lines. <i>A.Tourovsky, A.N. Schreuder, and E.A. de Kock</i>	33
Determination of the energy spectra used for proton therapy at the NAC. <i>M. R. Nchodu, F. D. Brooks, D. T. L. Jones, A. Buffler, M. S. Allie, P.J. Binns, J. E. Symons and J. V. Siebers</i>	33
Sacral chordomas treated with neutron and proton therapy. <i>S. Schroeder, and J. A. Wilson</i>	34
Treatment of adenoid cystic carcinoma of the trachea with neutrons. <i>J. Waggie, S. Rhoda, C. E. Stannard</i>	34

## Development of a scanning system for proton therapy in Uppsala.

S. Lorin<sup>1</sup>, N. Tilly<sup>1,3</sup>, J. Medin<sup>1</sup>, M. Blom<sup>4</sup>, V. Ziemann<sup>5</sup>, B. Glimelius<sup>1</sup> and E. Grusell<sup>2</sup>, <sup>1</sup>Section of Oncology, Uppsala University, <sup>2</sup>Section of Hospital Physics, Akademiska sjukhuset, Uppsala, <sup>3</sup>Department of Medical Radiation Physics, Stockholm University, <sup>4</sup>Department of Radiation Sciences, Uppsala University, <sup>5</sup>The The Svedberg Laboratory, Uppsala University, Sweden.

The scanning head, developed at the The Svedberg Laboratory (TSL) in Uppsala, enables full three-dimensional scanning of a 180 MeV proton beam with small polegaps and a moveable second magnet which is put into a cradle which has its rotational center in the first magnet. Since the polegap of the magnets in the present design is only 1.0 cm, the magnets can be small with a size of only 280 x 386 x 200 mm<sup>3</sup>. The magnetic fields in the magnets are 1.8 T which for a proton beam of 200 MeV and a SSD of 1 m yields a fieldsize of 300 x 300 mm<sup>2</sup>. This scanning head can be combined with a very compact gantry not considerably larger than gantries used for conventional treatments with photons and electrons.

The current in the first magnet determines the deflection angle and exit position of the beam from it. By a proper design of the polegap of the first magnet, the chosen current always correspond to a certain position of the second magnet resulting in a beam which is in the center throughout the polegap of the second magnet.

During the scanning procedure the mechanical motion of the second magnet has to be synchronised with the magnetic deflection of the beam in the first magnet. Therefore the vertically deflecting second magnet yields the fastest scan and the mechanical positioning and thereby the horizontal magnetical deflection of the beam in the first magnet yields the second fastest scan. This means that even for a very high pulse frequency of the cyclotron, the speed of the mechanical movement of the second magnet from one side to the other is rather slow, with a total time of a couple of seconds.

To position the Bragg peak at the specified depth, a range modulator is placed directly after the second magnet. It consists of eight Plexiglas slabs where the thinnest slab is 1 mm. They are arranged in a binary system so that the thickness of two adjacent slabs, except for the thickest one having a thickness of 73 mm, are duplicated, resulting in a total thickness of 200 mm. These slabs are then, in different combinations, pushed into the beam by pneumatic valves. This range modulation is carried out after that the magnetic scan at each depth is finished and is consequently the slowest part of the scanning procedure.

A software package, including an active steering system and a control system implemented on independent computers was developed. The control system is complex as it must contain several separate systems to assure full control of the treatment even if one of them should break down. For each pulse from the cyclotron, several parameters are read out such as the currents in the magnets, the position of the second magnet, the charge of the proton pulse from the ion source, the triggering frequency of the pulses from the cyclotron and the vertical position of the beam. These parameters are then compared to precalculated values, and if any deviation is found, which can not be compensated for during the scan, the treatment will be interrupted. The treatment can then be continued later from where it was interrupted since the parameter values are continuously stored in a log-file.

Automatic alignment of the beam through the scanning head is accomplished using two four-segment transmission ionisation chambers, where the first one is positioned in front of the scanning head and the other is mounted directly behind the second magnet. A dosimetry set up consisting of a duplicated pair of transmission ionisation chambers positioned before and after the scanning head has also been constructed and carefully calibrated to a Faraday cup. To monitor the vertical position of the beam after the last magnet an ionisation chamber divided in 24 segments was built and mounted behind the second magnet.

\*\*\*\*\*

## **Experience of 3-D proton beam spot scanning at NIRS.**

K. Kawachi and T. Kanai, National Institute of Radiological Sciences, Chiba, Japan.

Recently, many institutions are trying various type of beam scanning techniques for the charged particle therapy. This paper was described on the experience of 3-D proton beam spot scanning which was completed at NIRS medical cyclotron in 1981 (1). We had been applying 2-D proton beam spot scanning to the superficial tumor therapy since 1979 (2), however we had not a chance to apply 3-D proton beam spot scanning to the patient treatment.

The beam scanning system consisted of two orthogonal bending magnets, large area transmission type parallel plate ionization chamber and a computer controlled variable thickness absorber. The proton beam was 70 MeV and collimated 1cm square spot beam at the patient site. The experimental results were confirmed by the use of films and a multi-wire ionization chamber. Several results convinced us this technique has been useful in future for the charged particle therapy.

References: (1) K. Kawachi, T. Kanai, H. Matsuzawa, T. Inada, Acta Radiol. Suppl. (Stockh) 364, 81-88, (1983). (2) T. Kanai, K. Kawachi, Y. Kumamoto, H. Ogawa, T. Yamada, H. Matsuzawa, T. Inada, Med. Phys. 7, 365-9, (1980).

\*\*\*\*\*

## **Quality control of neutron beam: a cooperative study of ECHED.**

N. Iborra-Brassart<sup>1</sup> on behalf of ECHED, <sup>1</sup>Centre Antoine-Lacassagne, Cyclotron Médical, Nice, France.

The quality control of equipment results in optimising the treatment of patients. Quality assurance procedures are used in Radiotherapy for some years and were developed for <sup>60</sup>Co and electron accelerators. Only the determination of absorbed dose has been treated specifically for neutrons (ICRU 45). Regarding neutron equipment we are confronted with both the small number of facilities and their great differences. The main reaction used to produce a neutron flux is to bombard protons or deuterons on a Beryllium target and most of the installations are based on cyclotrons. The machine quality control has to be treated elsewhere. Regarding only neutron therapy equipment and the treatment room we find great similarities with electrons accelerators. So, we can adapt with some modifications, the recommendations of national and international protocols to neutron equipment. ECHED purpose will be to point out the particularities of neutron equipment so as to provide the necessary modifications to the existing electron accelerators procedures. A review of the quality control criteria was made from the documents received from some neutron installations, underlining the mains differences. For those criteria differing from standard procedures but usual with neutrons installations, ECHED has to describe simple, fast and reproducible measurements techniques and to give tests frequency and tolerance. These modifications may constitute a reference to be added to existing procedures to set-up a common basis for our specific installations of neutrontherapy. ECHED may propose references for the following criteria: - personnel radioprotection: background level in the room and activation levels for accessories and collimators, - mechanical parameters: geometrical field size indication, - neutron beam characteristics: definition of a quality index for the neutron beams, specification of a reference depth for the control of field flatness and symmetry as for the coincidence of light and irradiated field, - the gamma component: specific to neutron beams, it influences the absorbed-dose distribution in patients and has to be specified at different depths and off axis distances for various field sizes, - dose monitoring system: two systems are used, the target current or the ionisation through two parallel plate chambers. The last one is widely used for electron accelerators and the verifications are well described, - what place for microdosimetry which is another method to specify radiation quality in neutron therapy?

\*\*\*\*\*

**Design considerations for a computer controlled multileaf collimator for the Harper Hospital fast neutron therapy facility.**

R. L. Maughan<sup>1</sup>, M. Yudelev<sup>1</sup>, J. D. Forman<sup>1</sup>, E. B. Blosser<sup>2</sup>, S. B. Williams<sup>3</sup>, D. Gries<sup>3</sup>, W. Chapman<sup>3</sup>, and T. M. Fletcher<sup>3</sup>,  
<sup>1</sup>Gershenson Radiation Oncology Center, Karmanos Cancer Institute, Harper Hospital and Wayne State University, 3990 John R., Detroit, Michigan 48201, USA, <sup>2</sup>MedCyc Corporation, 1393 Hickory Island Drive Haslett, Michigan 48840, USA, <sup>3</sup>Williams International, 2280 West Maple Road, P.O.Box, 200, Walled Lake, Michigan 48390-0200, USA.

Since 1991 the Harper Hospital fast neutron therapy facility has used a unique multirod collimator (MRC) for creating irregularly shaped irradiation fields. Although this device has operated well in the clinical setting it does have some limitations; in particular it requires manual operation which is time consuming. Since, the neutron facility is at full capacity this can be problematic and it is estimated that patient throughput could be increased by 50% if the MRC was replaced with a computer controlled multileaf collimator (MLC). The mechanical complexity of an MLC can be considerably reduced if unfocused collimator leaves are used. The MRC is an ideal device for investigating the effects of the collimator leaf geometry, since the polystyrene blocks used to create the fields can be cut in such a way as to provide either focused or unfocused collimation. The effects of the shape of the collimator leaf on the beam penumbra measured in lateral beam profiles has been investigated as a function of field size and depth in a water phantom. When combined with in-air measurements it is possible to ascertain how factors such as leaf geometry, neutron source size, head scatter and phantom scatter contribute to the penumbra. The proposed MLC will have 120 leaves each with a 0.5 cm projection in the plane of the isocenter; the maximum field size will be 30 cm x 30 cm. Each leaf will be capable of traveling 8 cm beyond the center line of the field as measured at the plane of the isocenter. It is planned to use 30 cm thick iron leaves.

\*\*\*\*\*

**Program for the optimization of multiblade trimmer blade positions.**

C. van Gend, E. A. de Kock, and A. N. Schreuder, National Accelerator Centre, P O Box 72, Faure, 7131 South Africa.

A multiblade trimmer has been installed on the NAC neutron gantry, to improve the beam shape produced by the main collimator jaws. Positioning is achieved by using compressed air to push the blades against a pre-cut wooden core. The relatively thick (1cm) leaves cause however an unavoidable staircase effect at the field edge, resulting in unwanted radiation outside the treatment area. A program has been written to find the optimum blade angle so that this is minimised. The program furthermore allows the blade positions to vary so that there is a balance between overexposure outside and underexposure inside the irregular field outline, the weighting of each being determined by the clinician. A graphical user interface allows the final positions and angle to be checked visually, and the core calculation routines have been incorporated into the neutron planning system. Finally, the program produces a modified outline which may be used to cut the wooden core.

\*\*\*\*\*

**Microdosimetric response of carbon and oxygen in a p(66)/Be(40) THERAPY beam.**

P. J. Binns and A. N. Schreuder, National Accelerator Centre, P O Box 72, Faure, 7131 South Africa.

The international dosimetry protocol for neutron adopted by NAC recommends a kerma ratio of 0.95 between muscle tissue and A-150 plastic the material from which tissue equivalent chambers are usually constructed. The largest uncertainty in the estimation is the inexact knowledge of the varying kerma coefficients versus neutron energy.

In an attempt to improve the accuracy of dosimetry a direct determination of the neutron kerma for A-150 plastic and the constituent elements carbon and oxygen was performed under clinical irradiation conditions. Integral measuring techniques using low pressure proportional counters with walls made of different materials were applied. Using the obtained elemental microdosimetric responses those for muscle tissue and other tissue types relevant to therapy are synthesised by simple scaling. Dosimetric quantities as well as possible quality variations between different tissue types will be presented.

\*\*\*\*\*

**Progress report on the BNC enhancement studies at the Seattle fast neutron therapy beam and other developments.**

R. Risler<sup>1</sup>, G. E. Laramore<sup>1</sup>, K. S. Stelzer<sup>1</sup>, D. W. Nigg<sup>2</sup>, C. A. Wemple<sup>2</sup>, J. K. Hartwell<sup>2</sup> and Y. D. Harker<sup>2</sup>, <sup>1</sup>University of Washington, Seattle, USA, <sup>2</sup>Idaho National Engineering and Environmental Laboratory, Idaho Falls, USA.

An experimental neutron production target has been designed, built and tested with the goal of creating a neutron spectrum in the therapy beam, which will essentially have the same depth dose characteristics as the existing fast neutron beam, but will have a larger low energy tail resulting in an increased tumor dose, if a neutron capture enhanced treatment is utilized. The new target delivers roughly a 70% increase for the boron enhancement at clinically relevant depths for a 10 x 10 cm field. However, this improvement has been achieved at the cost of a 33 % dose rate reduction for a fixed proton beam intensity on target.

The new target is being clinically tested in the treatment of spontaneous lung tumors in dogs using the fixed beam unit of the facility.

A protocol for treating glioblastoma patients with the standard fast neutron beam using radiosurgery techniques has been approved. This work is based on local dose escalation experience using conformal photon radiation. Fluorodeoxyglucose positron emission tomography is used to delineate the final target volume. The treatment of the first glioblastoma patient is imminent. If the results of this trial are encouraging, it is expected to lead to a future randomized trial using a BNC enhanced beam.

\*\*\*\*\*

## **Dosimetry studies for boron neutron capture therapy and the feasibility of boron neutron capture enhanced fast neutron therapy at the Gershenson Radiation Oncology Center.**

R. L. Maughan, C. Kota, J. W. Burmeister and J. D. Forman, Gershenson Radiation Oncology Center, Karmanos Cancer Institute, Harper Hospital and Wayne State University, 3990 John R., Detroit, Michigan 48201, USA.

Miniature Rossi type tissue equivalent proportional counters for use in the epithermal neutron beams used for BNCT have been constructed. A miniature counter is required to prevent pulse pile up and saturation in the high flux beams used for therapy. A pair of counters is used in BNCT measurements; one counter has walls fabricated from A150 tissue equivalent plastic (TEP) while in the second counter the A150 TEP wall material is loaded with 200 ppm of  $^{10}\text{B}$  ( $^{10}\text{B}$ -A150). From measurements made with the two counters it is possible to determine the gamma ray, fast neutron, and boron neutron capture dose components. The response of the has been exhaustively characterized using a  $^{252}\text{Cf}$  neutron spectrum and the d(48.5)+Be fast neutron beam. These counters have been used to make dosimetric measurements in head-sized acrylic phantoms in the reactor produced clinical epithermal neutron beams at MIT and BNL. Preliminary results of these intercomparison measurements will be presented.

The feasibility of developing a modified fast neutron beam suitable for BNCEFNT has also been under investigation. A possible clinical arrangement involves moderating/filtering the existing fast neutron beam with 25 cm of steel. To ascertain the clinical usefulness of the beam it is necessary to produce a meaningful treatment plan for this form of therapy. One way of creating such a plan would be to use an algorithm based treatment planning method. To implement such a treatment planning system requires depth-dose scans and beam profile scans in a phantom for each of the three dose components. A pair of magnesium and  $^{10}\text{B}$  loaded-magnesium ionization chambers has been constructed; when scan information from these is combined with data from an A150 TEP ionization chamber it is possible to unfold gamma ray, fast neutron, and boron neutron capture dose scans separately and use them in an algorithm based treatment planning system.

\*\*\*\*\*

## **TLD-600 and TLD-700: a possible way to measure the thermal component in a fast neutron beam.**

N. Iborra-Brassart<sup>1</sup>, J. P. Pignol<sup>2</sup>, J. Herault<sup>1</sup>, P. Chauvel<sup>1</sup>, <sup>1</sup>Centre Antoine Lacassagne, Cyclotron Médical, Nice, France, <sup>2</sup>Service de Radiothérapie, Hôpital du Hasenrain, Mulhouse, France.

Chips (3.5 x 3.5 x 0.9 mm) of  $^7\text{LiF}$  and  $^6\text{LiF}$  thermoluminescence dosimeters were used in this study to discriminate the thermal component in the fast neutron beam [p(60)+Be(44)] in Nice. A study of J.A.B.Gibson demonstrate that both are sensitive to  $\gamma$  and neutron with neutron efficiency relative to the efficiency for  $^{60}\text{Co}$   $\gamma$  ray almost constant for neutron energies below 10 MeV. This constancy extends down to intermediate energies and down to 0.025 eV for TLD-600 which are sensitive to thermal neutrons. For  $^7\text{LiF}$  this neutron efficiency increases of a factor of 2 for neutron energy greater than 10 MeV.

The TLD-600 used in this study are enriched with 95.6% of Li-6 with a thermal cross section of 945 barns. The reaction  $^6\text{Li}(n,\alpha)^3\text{H}$  with the high ionizing  $\alpha$  particle explains the high efficiency of TLD-600 to thermal neutron. On the opposite TLD-700 contain only 0.007% of Li-6 and 99.993% of Li-7 with a thermal cross section of only 0.033 barn. So it is possible, by subtracting the response of a set of TLD-600 and TLD-700 irradiated simultaneously, to appreciate the thermal component in a fast neutron beam. All the measurements where made in a Plexiglas phantom.

The thermal neutron component increases with field size. Depth dose curves of thermal neutrons with 5x5, 10x10 and 20.5x22 fields sizes show a maximum at 8cm depth while the maximum depth for the fast

neutron beam is at 1.8cm measured with ionization chamber. At this maximum the thermal tld response of a 10x10 field is 3.2 higher than for a 5x5 and 2.4 less than for a 20.5x22 field. The thermal neutron component decreases slowly outside the field limit. For a 10x10 field the relative lecture for thermal neutron at 5cm from the beam axis is 75% against 50% for the fast neutron component.

To increase the thermal component while irradiating a small field, we reduced the maximum possible field size at the collimator to the desire field by using additional collimator of iron or lead blocks close to the surface of the phantom.

The ratio of thermal to fast neutron increases from 6, for a 10x10 field given by the multi-leaf at 20cm from the phantom surface, to 16, 17 and 18 for the same field obtained from the 20x22 field, collimated respectively by 10cm iron block, 5cm and 10cm lead blocks positioned on a wood support at 1cm from phantom surface. At 10cm depth this ratio increases to 8 for a 10x10 field at the multi-leaf while it is slightly decreasing to 15, 16 and 17 in the others experimental configurations. At 5cm depth, referring to a 10x10 field at the multi-leaf, the enhancement of thermal flux is respectively 146%, 160% and 173% for the three additional collimations mentioned above. These preliminary results demonstrate that tlds offer an interesting way to get, in a solid phantom, a distribution of thermal neutron flux under a fast neutron beam in different conditions. It will be relevant to confront in the same conditions, tlds results with those obtain with boron ionization chambers.

\*\*\*\*\*

### **Reliability of the micronucleus assay for predicting radiosensitivity.**

J. M. Akudugu, J P. Slabbert<sup>1</sup>, A. Serafin, and L. Bohm, Department of Radiation Oncology, Faculty of Medicine, University of Stellenbosch, P.O. Box 19063, Tygerberg 7505, South Africa, <sup>1</sup>National Accelerator Centre, P. O. Box 72, Faure 7131, South Africa.

It is generally assumed that radiation-induced micronuclei (mn) in cytokinesis-blocked cells are an expression of cellular radiosensitivity. Therefore radiosensitive cells should show a high frequency of mn and radioresistant cells should show lower levels.

We have irradiated a panel of thirteen neuronal cell lines of widely differing radiosensitivity (human neuroblastomas: n2 $\alpha$ , shsy5y, sk-n-sh, kelly and sk-n-be(2c); murine neuroblastomas: op-6 and op-27; human glioblastomas: g120, g60, g28, g112, g44 and g62) and compared their radiation response using the micronucleus and standard clonogenic assays. It was found that mn frequency was much higher in some of the radioresistant cell lines (n2 $\alpha$ , g28, g120 and g44; sf2  $\geq$  0.60). These cell lines showed a high mn frequency of more than 0.32 mn per gy of <sup>60</sup>co  $\gamma$ -irradiation per binucleate cell. On the other hand, the more radiosensitive cell lines (op-27 and sk-n-sh, sf2  $\leq$  0.27) produced 0.08  $\pm$  0.01 and 0.04  $\pm$  0.01 mn per gy, respectively. Op-6, sk-n-be(2c), g112, g62, g60 and kelly constituted an intermediate group and displayed a mn formation index between 0.10 and 0.24 mn per gy per binucleate cell. Shsy5y cells showed no detectable mn formation. In two groups (op-6, sk-n-be(2c), g112, g62, n2 $\alpha$  and g28 or g120, g60, op-27 and sk-n-sh) the more resistant cell lines produced more mn per unit dose. Another group (op-6, sk-n-be(2c), g112, g62, g44 and g120) produced no correlation at all between mn formation and radiosensitivity.

We conclude that the relationship between cell survival and mn formation is not straightforward and that it would be simplistic to translate mn frequency into radiosensitivity.

\*\*\*\*\*

## Comparison between dna and cytogenetic damages in lymphocytes from healthy donors and skin cancer patients.

A. Cebulska-Wasilewska<sup>1</sup>, W. Dyga<sup>1</sup>, S. Krasnowolski<sup>1</sup>, A. Wierzevska<sup>1</sup>, and E. Budzanowska<sup>2</sup>, <sup>1</sup>Department of Radiation and Environmental Biology, H. Niewodniczanski Institute of Nuclear Physics, 31-342 Krakow, Poland, <sup>2</sup>L. Rydygier Hospital, Department of Dermatology, Os. Zlotej Jesieni 1, 31-826 Krakow, Poland.

Individual susceptibility to the induction of DNA damage by radiation and cellular repair capability can be important factors affecting radiation therapy. There is also a lot of interest in the studies that would help to understand whether there is a causal association between cancer and various types of the molecular or cytogenetic damage detected in human cells. One major oncogenesis process is activation of proto-oncogenes by point mutations or chromosomal translocation. There is substantial evidence that indicates that loss of heterozygosity of certain chromosomes is involved in human carcinogenesis. Our study aimed to elicit the possible association between cancer and biomarker levels (DNA and cytogenetic abnormalities) detected in lymphocytes of persons bearing various categories of skin cancer cells, or with their individual capability to repair damage induced. Fresh blood was collected by venipuncture from 25 healthy donors and nine skin cancer patients prior to treatment. All patients were nonsmoking males, however 42.3 % of them were former smokers. Blood samples were divided into two parts and in the first part of samples cytogenetic studies were performed immediately, while from the second part lymphocytes were isolated and stored at - 70<sup>0</sup>C for further studies *in vitro*. In the latter one a single cell gel electrophoresis assay (SCGE) known as a Comet assay was performed to study individual susceptibility to the induction of DNA damage by UV or X-ray radiation and cellular repair capability. An average of 220 per sample of good metaphase spreads in the first mitotic division, and 100 per sample in the second division, were accepted for the analysis of cytogenetic damage. Chromosome and chromatid type aberrations were scored in the cells in the first mitosis and expressed as total aberration frequency including gaps and excluding gaps. Sister chromatid exchanges, high frequency cells and proliferate rate index were screened and evaluated in the second mitosis. Each of the skin cancer patients revealed a significant increase in at least one of the cytogenetic biomarker levels comparing level in the reference group. In order to estimate individual susceptibility to the induction of the damage by environmental agents, the isolated lymphocytes were irradiated with UV or X-radiation and DNA damage was detected with an application of the single cell gel electrophoresis (SCGE assay) also known as COMET assay. The lymphocytes were isolated from 0.5 ml of blood from each patient, irradiated with 2 Gy dose of X-rays or 6 J/m<sup>2</sup> of UV radiation and the SCGE was performed. To compare various individual capabilities to repair damages induced incubation of cells in presence or absence of cellular processes starting agent was also done prior to DNA damage analysis. Statistically significant higher response to UV, with significantly lower variability in repair capabilities in skin cancer patients were observed. Significantly higher on the average response to X rays, and lower capability to repair DNA damage in skin cancer patients than in healthy donors was observed. Variability in radiosensitivity of the cells from healthy donors and skin cancer patients is discussed. Acknowledgment: Research was partially supported by contracts of the State Committee of Research KBN No6P04A05112, and Commission of the European Communities ERBIC 15CT960300.

\*\*\*\*\*

## Proton irradiation and dose-volume effects in the rat spinal cord.

H.P. Bijl<sup>1</sup>, A.J. van der Kogel<sup>2</sup>, P. van Luijk<sup>3</sup>, J.M. Schippers<sup>3</sup>, R. Coppes<sup>4</sup>, B.G. Szabó<sup>1</sup> and A.W.T. Konings<sup>4</sup>, <sup>1</sup>Department of Radiotherapy, University Hospital of Groningen, <sup>2</sup>Department of Radiotherapy, University Hospital of Nijmegen, <sup>3</sup>KVI, University of Groningen, <sup>4</sup>Department of Radiobiology, University of Groningen, The Netherlands.

The purpose of this study is to estimate the dose-volume effects in the rat spinal cord with protons and to investigate the development of normal tissue damage with MR imaging followed by light microscopy analysis.

**Materials and methods:** Wistar rats were irradiated on the spinal cord (region C1-T2) with a single fraction of unmodulated protons (150-200 MeV), using the shoot through method. Three different length of the spinal cord were irradiated (4, 8 and 20 mm) with the center of the field at C4.

To investigate the influence of migrating glial stem cells on the ED50 for small volumes, a top-up experiment was performed in which 20 mm of the spinal cord was irradiated at a sub-threshold dose (18 Gy) in combination with variable doses to a length of 4 mm at the center. The endpoint for estimating ED50 values was paralysis of fore and/or hind limbs.

Two distinct pathological tissue lesions may be seen after irradiation of the spinal cord namely white matter necrosis and gross vascular abnormalities. In vivo Magnetic Resonance spin-echo experiments (7 T, TE=25 mm, TR=2500 mm, FOV=40 mm, matrix size=256x256, slice thickness=0.5 mm) were performed to detect abnormalities in irradiated segments of the spinal cord. The MR-images will be compared with light microscopic analysis of the same segment of the spinal cord.

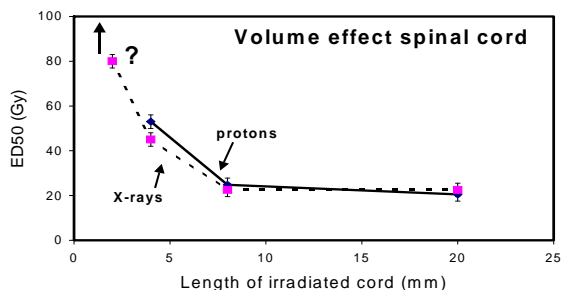


**Figure 1.** Dose at which 50% of the animals show paralysis, as a function of irradiated cord length.

**Results:** The initial results obtained for protons are similar to those obtained previously for 4-6 MV photons (Fig. 1), showing a marginal increase of ED50 when decreasing the cord length from 20 to 8 mm, but a steep increase in ED50 when further decreasing the length to 4 mm. At the higher ED50's, the latent period to paralysis decreased. In the top-up experiment, the ED50 at 4 mm was reduced compared to the irradiation of a 4 mm field only. The MR-images provided an excellent contrast between grey and white matter and clearly showed the radiation induced damage in the spinal cord.

**Conclusions:** The similar ED50 values for photons and protons at 8 and 20 mm indicate that the RBE of plateau protons is close to unity. The difference in ED50, for photon and proton irradiation at 4 mm, can probably be explained by differences in dose distribution. A decreased ED50 in the top-up experiment suggests an impaired migration of target cells. MRI seems to be a useful tool for in vivo assessment of radiation induced damage to the spinal cord.

\*\*\*\*\*

### **Treatment planning of eye tumors: problems encountered.**

N. Iborra-Brassart, J. Herault, PY. Bondiau, A. Courdi, and P. Chauvel, Centre Antoine-Lacassagne, Cyclotron Médical, NICE – France.

From June 1991 to March 1999, 1300 patients were treated in Nice for an ocular disease using the 65 MeV proton beam of the Medicyc cyclotron. For all patients the Eyeplan treatment planning software was used. Two main problems are presently unsolved in Eyeplan.

The first problem to be solved is the eyelid's shape, thickness and position in the beam which are very difficult to reproduce from one day to another. If the lids are taken off the beam by using retractors, their retraction has to be really complete. If not, the lid remaining in the beam gives a relief looking like a stair which may vary from one day to another. This would lead to an underdosage of part of the target volume or an overdosage of a critical structure. Moreover, irradiation of the lid margin would bring about the loss of eyelashes. If the lid(s) can't be completely withdrawn from the beam it is better to pull the lid in and ensure a good protection of the rim and eyelashes. But this doesn't solve the problem of the reproducibility of shape, thickness and position. In addition some parts of the lids, as the internal canthus, can't be moved apart and their relief will remain as stairs in the beam. Depending upon the choice of the reference point for the estimate of eyelid thickness and even using the tools designed in Eyeplan to draw and take into account the lids, we should experience either a risk of underdosage of a part of the tumor volume or an excessive irradiation of a critical structure due to the daily repositioning. These considerations led us to describe and set-up the use of bolus (tissue compensator put on the skin surface) permitting to obtain a plane entrance perpendicular to the beam (whatever could be the status of the eyelid) corresponding to the Eyeplan basic lid calculation. Initially it was carved out of wax and interfaced to the eye and lid with ultrasonographic gel (USG). Soon wax was replaced by only USG and a thin piece of a transparency film allowing to flatten the bolus.

The second problems deals with the eye modelization which does not always fits with the real eye anatomy. Eyeplan cannot display any other modelization than spheres and eye is not frequently spherical. We are presently performing a CT scan for each patient, treat it in a standard radiotherapy TPS (ISIS 3D) in order to obtain a virtual simulation of the eye in beam's eye view, lateral view and overview. These views are superimposed to those obtained from the Eyeplan model orientated in the same position as the eye during the CT scan. This allows to perform some modifications of the model allowing to better represent the real eye or at least the treated area. But a reliable 3-D reconstruction of the eye and tumor which could be incorporated in the treatment planning system in order to represent accurately any eye shape has to be implemented. A research project is in progress in collaboration with the INRIA (Institut National de Recherche en Informatique et Automatisation) in view of combining the information coming from CT, MRI and fundus photographs. The feasibility study is achieved and clearly demonstrates the usefulness of the method for eye modelization. A friendly user version is now in progress to allow a routine use of this automatic modelization. The incorporation of such a model in a treatment planning system will enhance the present possibilities of protontherapy to deliver a well targeted dose distribution. This will be the last step of this research program partly granted by the south east French Cancer League.

\*\*\*\*\*

## Uveal melanomas: results of protontherapy in Nice.

P. Chauvel, A. Courdi, JP. Caujolle, JD. Grange, L. Diallo-Rosier, J. Sahel, F. Bacin, C. Zur, N. Iborra-Brassart, J. Herault, and P. Gastaud, Centre Antoine-Lacassagne, Cyclotron Médical, NICE – France.

**Material and methods:** From June 1991 to December 1996 538 uveal melanomas were referred by the French ophthalmology teams cooperating with the Medical Cyclotron in Nice. They were treated by 65 MeV protons produced by the Medicyc cyclotron. The tumor parameters were measured using ultrasonography and angiography. Since 1994, CT scans were performed in most patients to help precise the axial length and the shape of the ocular globe. Tantalum clips were inserted around the tumor before referral. Tumor site was posterior pole for 64.9%, equatorial for 24.1%, and ciliary body for 11%. There were 7.5% T1, 30.5% T2, 60.2% T3 and 1.8% T4 tumors. The median tumor thickness was 5 mm. The tumor construction and the dosimetry were executed with the EYEPLAN software. All patients received 52 Gy (60 Gy Co-equivalent dose) in 4 consecutive days. The data were analyzed by December 1997.

**Results:** The median follow-up was 32 months. At the end of the study, 56 patients were dead, and the Kaplan-Meier overall survival (OS) was 74.2% at 6.5 years. The recorded site of the tumor had no significant influence on patient survival: patients with ciliary body tumors had an OS of 85.7%, not significantly different from other tumors: 73.7%. The tumor size significantly affected OS: for T1 and T2 lesions it was 79.9%, versus 71.0% for T3 and T4 tumors ( $p = 0.009$ ). Patients with tumor thickness above the median value tended to die early; however the OS at 6.5 years was not significantly influenced by tumor thickness ( $p = 0.085$ ). At closure of the analysis, 43 metastases were observed (8%), 38 of them were located in the liver. The metastatic rate was 3.9% for T1 and T2 lesions, versus 10.4% for T3 and T4 lesions ( $p = 0.007$ ).

The Kaplan-Meier local control (LC) was 89% at 6.5 years, the rate of eye conservation was 88%, and the disease free survival (DFS) was 78%. LC was 98% for T1 and T2 vs 84% for T3 and T4 ( $p = 0.003$ ). Tumors with below median thickness had better LC ( $p = 0.0006$ ), as well as tumors with below median diameter ( $p = 0.007$ ). Size and thickness also affected enucleation rate and DFS. Neither LC, eye conservation nor DFS was dependent on the tumor site.

Visual acuity prior and after treatment was evaluated in 284 patients. Of these, 33.5% had a stable or an improved vision. 50.4% of patients retained a useful vision ( $\geq 20/200$ ).

**Conclusion:** Patient survival and metastatic rate are mostly affected by the T stage of the tumor. Tumor size, but not its site, significantly affects the prognosis. Although the majority of referred tumors were advanced (T3 or T4), survival of these patients compares favorably with other treatment alternatives. In addition, a useful vision can be offered in a substantial number of patients.

\*\*\*\*\*

## Proton Beam Therapy for Age-related Macular Degeneration: Development of a Standard Plan.

J. A. Adams<sup>1</sup>, K. L. Paiva<sup>1</sup>, J. E. Munzenrider<sup>1</sup>, J. W. Miller<sup>2</sup>, and E. S. Gragoudas<sup>2</sup>, <sup>1</sup>Department of Radiation Oncology, Massachusetts General Hospital, Boston, MA 02114, <sup>2</sup>Retina Service, Massachusetts Eye and Ear Infirmary, Department of Ophthalmology, Harvard Medical School, Boston, MA 02114

Age-related macular degeneration is the leading cause of blindness in developing countries. Irradiating the exudative form in which a choroidal neovascular membrane develops in the sub-foveal area (SCNV) is presently a treatment under investigation. In 1995 Massachusetts General Hospital collaborating with Massachusetts Eye and Ear Infirmary initiated a protocol to treat SCNV membranes using the proton beam at the Harvard Cyclotron Laboratory and the EYEPLAN program with a light field setup. EYEPLAN requires the axial eye length, membrane dimensions, and manipulation of the eye to include a

4.0 mm radial margin around the membrane so that the aperture margin (50% isodose line on the posterior retina) abuts the inferior aspect of the limbus. Review of 100 individually prepared plans showed that 95% of the fabricated apertures were circular (aspect ratio <1.095) with diameters 9.5mm to 15.0mm. This information was used to develop an automated standard plan. Thirty nine plans were developed for axial lengths ranging from 21.0mm to 25.0mm and membrane sizes from 1.5 mm to 6.75 mm in the usual way as the reviewed ones. Circular targets were outlined centered on the fovea. Distal and proximal 90% ranges (modulation) to the target and doses to macula, optic disc, lens, ciliary body, retina and globe were calculated. An automated standard plan requiring the same input data but avoiding the need for individual plans was developed. The program outputs the aperture diameter, fixation angle for the light field setup, range and modulation, and calculates dose to the macula, optic nerve and percentage of retina receiving  $\geq 50\%$  and  $\geq 90\%$  of the prescribed dose. Individual plans require approximately 1 1/2 hours; the standard plan, 5 minutes. The standard plan could have treated 86% of the reviewed plans. The automated plan provides accurate and efficient treatment parameters for the majority of patients.

\*\*\*\*\*

### **The treatment of age-related macular degeneration using the Clatterbridge proton beam.**

A. Kacperek<sup>1</sup>, M. C. Briggs<sup>2</sup>, R. D. Errington<sup>1</sup>, S. P. Harding<sup>2</sup>, B. Jones<sup>1</sup>, M. A. Sheen<sup>1</sup> and J. Kongerud<sup>1</sup>, <sup>1</sup>Clatterbridge Centre for Oncology (CCO), Bebington, Wirral L63 4JY, UK, <sup>2</sup> St Paul's Eye Unit, Royal Liverpool Hospitals, Liverpool L7 8XP, UK.

Recent studies ARMD (age-related macular degeneration cases) using conventional fractionated external beam radiotherapy with narrow, oblique X-ray beams have indicated the beneficial effects of low doses of ionising radiation (1, 2) although patient numbers and follow-up period are still quite modest, and the prescribed dose regime is not definitive. However, the dose distribution patterns include sensitive parts of the eye such as the optic nerve and lens. The CT planning and the making of custom-made head restraint 'shells' create extra demands on radiotherapy resources.

The use of an existing proton beam facility, at the CCO cyclotron unit, would overcome these difficulties. The treatment schedules at the Unit allow minimal delay between diagnosis and treatment. The conformal characteristics of proton beams, with their sharp distal and lateral 'fall-offs', the simpler head restraint devices and planning requirements were considered to offer potential advantages over conventional radiotherapy (3).

A pilot study, which was transformed into a randomised study, was commenced in December 1997 using four, daily FX of 4.5 Gy. The treatment was simplified by use of circular collimators (lesion diameter + 3 mm radial safety margin) and field-light positioning. The total prescribed dose was informed by previous clinical experience with choroidal haemangiomas. Patients were entered in the study if they had: --

- 1) recent visual loss,
- 2) evidence of proven subfoveal CNVM using fundus fluorescein angiography (FFA),
- 3) life expectancy >1 year,
- 4) aged 50 years or over,
- 5) visual acuity of > 6/60. FFA would be performed on each patient at St. Paul's Eye Unit at 3 monthly intervals for at least 1 year. Patients were recruited from the Merseyside region and treated on an out-patient basis within a week of FFA.

The planning and setting-up technique will be presented with preliminary patient results.

References: (1) Chakravarthy U. et al. Treatment of age related subfoveal neovascular membranes by teletherapy: pilot study. *Brit. J. Ophthalmology* 1993 77: 265-73. (2) Hart P.M. et al. Teletherapy for subfoveal choroidal neovascularisation of age-related macular degeneration: results of follow up in a non-randomised study. *Brit. J. Ophthalmology* 1996 80: 1046-1050. (3) Yonemoto L.T. et al. Phase I/II study of proton beam irradiation for the treatment of subfoveal choroidal neovascularisation in ARMD: treatment techniques and preliminary results. *Int. J. Radiation Oncology Biol.Phys.* 1996 36: 867-871.

\*\*\*\*\*

### **Preliminary results of protontherapy in age related macular degeneration.**

P. Chauvel<sup>1</sup>, C. Zur<sup>2</sup>, JP. Caujolle<sup>2</sup>, N. Iborra-Brassart<sup>1</sup>, J. Herault<sup>1</sup>, N. Pinto<sup>1</sup>, A. Courdi<sup>1</sup>, and P. Gastaud<sup>2</sup>, <sup>1</sup>Centre Antoine-Lacassagne, Cyclotron Médical, <sup>2</sup>Service d'Ophtalmologie, CHRU - NICE – France.

Material and methods: From July 97 to June 98, 120 patients were treated for an age related macular degeneration (ARMD). Out of these 120, 58 were included in a controlled study, approved by ethic committee and health ministry. Inclusion criteria were: occult retrofoveal choroidal neovascularization (ORCNV) confirmed by indocyanine green angiography(ICGA), age>50 years, life expectancy > 2 years, visual acuity < 5/10. A single dose of 9.1Gy (10CGE) was delivered to the macular region by our 65 MeV proton beam, after a CT scan and a dosimetry on Eyeplan software. According to the protocol, the results were estimated at 3 and 6 months by measuring visual acuity: improvement was defined as initial visual acuity (IVA) plus > 2 lines, stabilization as IVA plus/minus 2 lines, worsening as IVA minus > 2 lines on EDTRS scale. Patients were treated in a sitting position with mask and byte block. The eye is turned 30 degrees polar on the nasal side using a red diode, in order to spare the anterior chamber and lens. The lack of movements during the treatment is checked through the same video system used for the treatment of uveal melanomas. 48 patients were evaluated at 3 months, 30 at 6 months and 6 at 1 year.

Results: The mean age was 78.2 years (66 to 90), 70.7% of patients were female. No problems were noted on eye or teguments at the first consultation, except for 2 patients presenting with a dry eye syndrome and 1 with a keratitis.

Mean intraocular pressure was 13.9 Hg mm (10 to 17). None of the patients developed acute or late morbidity related to the radiation treatment. 2 patients presented with visible feeder vessels. Only one more vessel appeared during the follow-up. 45% presented with hemorrhages: 27% remained stable, 73% decreased, no new hemorrhage appeared. 33% presented with exudates: 16% increased, 37% were stable, 47 % decreased, no new exudate appeared. 14% presented with macular cystoid oedema: 86% remained stable, 14% decreased, none appeared. 41% presented with sub retinal detachment : 5% increased, 75% were stable, 20% decreased, none appeared. 10% presented with fibrovascular pigment epithelial detachment : all remained stable, none appeared. 43% presented with metamorphopsies: 83% remained stable, 17% vanished, none appeared. No cataract related to treatment appeared. Near vision was improved or stabilized for 85.4% at 3 months, 80% at 6 months and 83.3% at 1 year. Distant vision was improved or stabilized for 87.5% at 3 months, 86.6% at 6 months and 83.3% at 1 year.

Conclusions: a single dose of 9.1Gy was efficient on ORCNV. The treatment tolerance was excellent. Visual acuity was stabilized or improved for more than 80 % of the patients without any adverse effect. A new randomized trial is now starting, comparing 3 levels of single proton dose (9.1, 10.9 and 12.7 Gy) aiming to underline a possible dose effect relationship. 200 patients will be included over 4 years.

\*\*\*\*\*

**Treatment of tumours of the nose, paranasal sinuses and orbit with neutron and proton therapy.**

C. Stannard<sup>1</sup>, J. Wilson<sup>1</sup>, A. O’Ryan<sup>2</sup>, S. Fredericks<sup>2</sup>,<sup>1</sup>Department of Radiation Oncology, Groote Schuur Hospital & University of Cape Town, <sup>2</sup>National Accelerator Centre, Faure

Inoperable tumours of the nose, nasopharynx, paranasal sinuses and orbit and those with macroscopic residual disease after surgery that could benefit from neutron therapy are compromised because of the proximity of the brain and optic chiasm and the unacceptable morbidity that full dose neutron therapy would have on these vital structures. Whilst giving full dose neutron therapy to most of the tumour we have boosted the low dose area adjacent to vital structures with fractionated proton therapy to maintain a radical dose to the whole tumour without undue morbidity.

Since 1994, 12 patients have been treated. Six had adenoid cystic carcinoma (ACC) or adenocarcinoma of the nose, nasopharynx or paranasal sinuses, 2 had squamous carcinoma of the maxillary antrum, 2 had adenoid cystic carcinoma of the lacrimal gland, one had a malignant melanoma of the nose and nasopharynx and one had an osteosarcoma of the orbit and maxillary antrum. In 8 patients the neutron dose was reduced to the tumour adjacent to vital structures by suitable shielding and this area was boosted with fractionated proton therapy. In 4 patients part of the treatment was given to the whole volume by neutron therapy supplemented by proton therapy to the whole volume.

There were 6 complete responses at 5-58 months (median 15 months), 2 partial responses at 9 and 15 months, progressive disease in 3 patients at 1 month (osteosarcoma), 7 months (squamous carcinoma) and 12 months (adenocarcinoma) and one patient was lost to follow up. The first patient treated thus with a CR up to 48 months had recurrent disease at 52 months.

Although these results are very preliminary, they are nevertheless encouraging in a group of patients who did not have any further options. The National Accelerator Centre (NAC) is the only centre in the world where both high energy neutron and proton therapy are available for patient treatment. It is therefore important for us to establish whether there is an advantage in combining the two modalities in selected cases.

\*\*\*\*\*

**The potential use of proton therapy in the management of craniopharyngiomas in children.**

J. L. Habrand, H. Mammar, R. Ferrand, C. Kalifa, Centre de Protonthérapie d’Orsay - BP 65, 91402 ORSAY - France

Craniopharyngioma is a benign but aggressive tumor that represents approximately 10 % of brain tumors in children and adolescents and 50 to 60 % of sellar ones. Most are seen between 7 and 13 years of age. Surgery represents the mainstay of treatment although complete resection is not always feasible and induces a high rate of complication (mainly related with hypothalamic and pituitary injuries). Incomplete resection appears safer but is followed by a local relapse in half cases. Following post op. irradiation, the risk is decreased further and possibly related with the total dose administered. We will present the rationale for using high dose protontherapy : dose-effect relationship from data in the literature, location in the base of the skull (close to highly sensitive structures), peculiar sensitivity due to young age of patients. Two cases treated at our institution will be presented.

\*\*\*\*\*

## **Proton fractionated stereotactic radiosurgery for secreting pituitary adenoma: the NAC experience.**

J. K. Harris<sup>1</sup>, F. J. A. Vernimmen<sup>2</sup>, J. Wilson<sup>3</sup>, M. Conradie<sup>4</sup>, <sup>1</sup>National Accelerator Centre, Faure, South Africa, <sup>2</sup>Dept of Radiotherapy, Tygerberg Hospital and Stellenbosch University, South Africa, <sup>3</sup>Dept of Radiotherapy, Groote Schuur Hospital and University of Cape Town, South Africa, <sup>4</sup>Endocrine Unit, Dept of Internal Medicine, Tygerberg Hospital and University of Stellenbosch, South Africa.

**Aim:** To determine the impact of fractionated stereotactic proton radiosurgery on the hormonal status of pituitary secretory adenomas and to determine the acute and late adverse effects of such treatment.

**Materials and Methods:** A retrospective review of patients with secretory pituitary adenomas treated at NAC between June 1994 and December 1998, was undertaken. During this time 29 secretory adenomas were treated: 6 patients were excluded from this analysis due to inadequate follow up (4 patients) or due to hyperfractionation (2 patients). The mean follow up time is 23.7 months (range 3-56 months). Three patients were treated by means of proton radiosurgery as sole modality; 20 patients had received prior surgical procedures. Two patients had received prior radiotherapy. Ten patients had received prior medical therapy. Of the 23 evaluable patients, 10 had Cushing's Disease, 11 had Acromegaly, 1 had a Prolactinoma and 1 had a TSH secreting tumor. The mean tumor volume was 1.9 cm<sup>3</sup> (range 0.3-5.5 cm<sup>3</sup>). The mean minimum total target dose was 40.7Gy (range 28.5-60) given in 3-4 fractions.

**Results:** Six of the 11 Acromegalic patients (54%) had growth hormone levels return to normal persistently within a mean time of 13.2 months. Eight of the 10 Cushing's patients (80%) had ACTH and/or 24hr urinary cortisol and/or 8am serum cortisol levels return to normal within a mean time of 15.5 months. The prolactinoma patient has persistently raised prolactin levels after 9 months of follow up. The patient with a TSH-producing adenoma had normal levels of TSH and T4 after 12 months of follow up. Acute and subacute adverse events were minimal and self-limiting. Moderately severe late effects were seen in 1 patient who had received prior radiotherapy in the form of cavernous sinus cranial nerve palsies and memory loss. Of the 15 patients who had intact anterior pituitary function prior to radiosurgery, one third required hormone replacement in 1-2 pituitary axes. Of the 4 patients who had pre radiosurgery deficiency in 1 pituitary axis, 2 resolved their deficiency and 2 developed progressive deficiency. All patients with preradiosurgery deficiency in 2 or more axes remained unchanged. There was no apparent visual pathway damage.

**Conclusion:** Stereotactic fractionated proton radiosurgery provides reasonable control for growth hormone-producing pituitary adenomas and effective cure for ACTH-producing pituitary adenomas. The time required for reduction of hormone levels is markedly less than for conventionally fractionated EBRT.

\*\*\*\*\*

### **Dose-volume relationships in radiosurgery.**

B. J. Smit, Dept. of Radiotherapy, Tygerberg Hospital, University of Stellenbosch, Private Bag, Tygerberg 7505, South Africa.

For the past three decades, efforts have been made to predict the neural implications resulting from single large doses of irradiation. Kjellberg (1986) drew "regression lines" representing a 1% risk of brain necrosis by plotting collimator diameter versus dose.

Flickinger (1991) took parameters like the prescription isodose into account and incorporating the data with a "logistic regression model" for a 3% risk of brain necrosis not unlike that of Kjellberg but nonetheless, by his own admission giving inconsistent results. Lax and Karlsson (1994) could relate complications to the received volume of 20 cm<sup>3</sup>. Flickinger (1997) found that the 12 Gy isodose line was an independent discriminant and volumes of 10 cm<sup>3</sup> receiving 10 Gy (minimum) would predict a

complication rate of 10% in the brain and 20% in the brain stem. Voges et al (1996) showed that the constraint of [10 Gy 10 cm<sup>3</sup>] of brain tissue predicted zero complications for linear accelerator based radiosurgery. Using this constraint as a point of departure for safe radiosurgery, a series of dose-volume tables were constructed taking *individual treatment parameters for each patient* into account, thus allowing a customized, index of dose-volume relationships for AVM's and skull base tumours, for comparison against the existing dose-volume models.

The tables are intended as an additional safety control mechanism to complement existing models. The tables show that the maximum volume of brain that can be irradiated safely, may have an upper limit of 10 cm<sup>3</sup>, and that the planning target volume together with the isodose defining the 10 Gy limit may serve as a guide to dose-volume relationships.

\*\*\*\*\*

### **High dose proton-photon therapy in the management of aggressive intra-cranial malignancies: update of the Orsay series.**

J. L. Habrand, H. Mammar, N. Gokarn, C. Haie, D. Pontvert, C. Lenir, R. Ferrand, A. Rey, and J. J. Mazon, Centre de Protonthérapie d'Orsay - BP 65, 91402 ORSAY - France

From October 1993 through July 1998, 48 evaluable adult patients with non resectable aggressive intra-cranial tumors were treated by a combination of high dose photon + proton therapy at the Centre de Protonthérapie d'Orsay. Grade 1 and 4 gliomas were excluded. Patients benefited from a 3D dose-calculation based on high definition CT and MRI, a stereotactic positioning using implanted fiducial markers and a thermoplastic mask. Mean tumor-dose ranged between 63 and 67 Gy delivered in 5 weekly sessions of 1.8 Gy in most patients, according to the histological types (dose in Co Gy Equivalent, with a mean proton-RBE of 1.1). With a median 18 month-follow-up (extr. 4 - 58 months), local control in tumors located in the envelopes and in the skull base was of 97 % (33/34) and in parenchymal tumors of 43 % (6/14). None of the 27 patients with BS chordomas - chondrosarcomas and only one of the 7 « aggressive » or malignant meningiomas has failed so far. Two patients (5 %) presented with a clinically severe radiation-induced necrosis (temporal lobe and chiasm). In our experience, high dose radiation combining photons and protons is a safe and highly efficient procedure in selected malignancies of the skull base and envelopes.

\*\*\*\*\*

### **The new energy degrading system for the NAC proton therapy beam.**

A N. Schreuder A. Kiefer, J. van der Merwe, A. Muller, K. Langen, and J. E. Symons, *National Accelerator Centre, P O Box 7131, Faure.*

A new energy degrading system was installed recently in the National Accelerator Centre (NAC) proton therapy beam line. The system consists of two identical carbon wedges that move in opposite directions across the beam axis. This ensures that the total thickness of carbon at a given time is uniform across the proton beam. The wedges are driven by a computer controlled stepper motor and their positions are verified by a V-binary position encoder. The wedge angle is 11.9 degrees and the wedges are 400 mm long. The wedges are installed in a "as far as possible" upstream position. This allows a beam spot of only 30 mm in diameter resulting in a minimum water equivalent wedge thickness of 20 mm. The double wedge system can degrade the beam in of 0.1 mm water equivalent steps.

In addition to the double wedge degrader a multi-layer Faraday Cup (MLFC), acting as a beam energy monitor was installed. The MLFC consists of 40 brass plates, each 0.5 mm thick, insulated from each other by 1 mm thick Lexan sheets. The Brass plates and Lexan sheets all have a 30 mm diameter hole in the centre which allows the monitor to be used as an anti-scatter collimator while the useful beam passes through to the patient. The monitor can therefore be used to interactively monitor the beam energy during treatments to correct for possible drifts in the incident beam energy.

Activation of the carbon is a problem especially during dosimetry measurements. This results in an unacceptable exposure rate at the position of the modulator propellor, which is located just downstream of the wedges. Since the modulator propellor needs to be changed manually, it was necessary to install a 30 mm steel radiation shield around the double wedge and MLFC systems to protect the operator during this procedure.

The energy resolution of the MLFC system is sufficient to resolve energy drifts corresponding to changes of approximately  $\pm 0.2$  mm in the water equivalent range of the beam.

\*\*\*\*\*

### **CT Scanner for imaging upright patients.**

A. J. Lennox and T. K. Kroc, Fermilab, MS 301, P. O. Box 500, Batavia, IL 60510-0500, USA.

In collaboration with Willard Productions, a commercially available GE-8800 computerized axial tomography scanner has been reconfigured to image patients in the sitting or standing position. The steel bearing assemblies supporting the imaging equipment in GE-8800 scanners were originally designed for use in army tank gun turrets. Hence, they are capable of maintaining a rigid horizontal plane on which the x-ray source and detectors rotate. Three Unilift screw jacks raise and lower the gantry to enable imaging at the desired elevations. The screw jacks are mounted on box-beam supports and are powered by a three horsepower motor. An interface module sends appropriate signals to the computer to facilitate scanning with no modification of the standard software. This paper presents a status report on the commissioning of the scanner for neutron therapy patient planning at Fermilab.

\*\*\*\*\*

### **A design of a compact gantry for proton therapy with 2D-scanning.**

H. Vrenken, R. Schuitema, O.C. Dermois and J. M. Schippers, Kernfysisch Versneller Instituut, 9747 AA Groningen, the Netherlands.

The reduction of size of proton gantries may increase the applicability of proton therapy in a clinical environment. Several attempts have been made to decrease the size (especially the radius) of gantries. The most compact gantry so far (developed at PSI), has been made by incorporation of pencil beam scanning into the ion optics of the gantry. Pencil-beam scanning by magnets is performed in one direction only and scanning in the orthogonal direction is performed by moving the patient couch. Also in other designs mechanical movements of couch and/or a magnet is employed to accomplish the orthogonal scanning direction. This is, however, substantially slower than a full magnetic scanning.

In this contribution we present a design of a compact gantry which allows fast pencil beam scanning in two orthogonal directions, so that a clinically relevant field of  $30 \times 30$  cm<sup>2</sup> can be irradiated without any mechanical motion of a component. In our design the pencil beam scanning is performed by two independently working scanning magnets. A compact system has been achieved by integration of the

beam scanning into the ion optical design of the gantry. The large deflections of the pencil beam from the optic axis of the gantry have been treated correctly by the ion optics code COSY. The ion optical design of the gantry and the use of COSY for the study of the action of the scanning magnets are discussed.

\*\*\*\*\*

### **Organ Motion.**

K. M. Langen, D.T.L. Jones, National Accelerator Centre, PO Box 72, Faure, 7131 South Africa

The patient's anatomy and position during the course of radiation therapy varies to some degree from the one used for treatment planning purposes. This is mainly due to patient movement, uncertainties in patient position and organ motion. The latter problem was approached by conducting a literature search for discussions and quantifications of organ motion as well as compensation methods.

Data were compiled and classified according to type of motion, i.e. motion between fractions and during irradiation. The former is associated with the digestive system and data were found on bladder, rectum and prostate movement. Organ motion during irradiation is mainly due to breathing and data were compiled for liver, diaphragm, kidney, lung tumors and pancreas. Techniques that are designed to compensate for organ motion such as radio-opaque marker implants and breathing gated irradiation were briefly reviewed. Lastly the relationship between clinical target volume margins and magnitude of organ motion was discussed.

\*\*\*\*\*

### **Improvements to the NAC proton position verification system.**

C. van Gend, E. A. de Kock, and A. N. Schreuder, National Accelerator Centre, P O Box 72, Faure, 7131, South Africa

The NAC proton therapy patient positioning system uses stereophotogrammetric (SPG) techniques to determine accurately the position of a set of markers (1 mm diameter steel balls) embedded in a close-fitting patient mask. The location of these relative to the tumour volume is extracted beforehand from the patient's CT data. These two data sets are then used to position the patient accurately in the beam, and the position may be verified by a portal X-ray image. The positions of the markers are digitized from this image, and these are then registered against the set of marker positions obtained from the SPG system, rotated and projected to the plane of the portal image. The distances between corresponding marker positions may then be calculated, and this is minimized in a least-squares fashion, varying the gantry and couch angles used to transform the SPG data. It is found that, although there are non-negligible separations between the measured and calculated positions, these are not reduced significantly by the least squares process. We conclude that these errors are likely to be caused by uncertainties in the marker positions obtained from the CT data, rather than patient mis-positioning by the SPG system.

\*\*\*\*\*

## Digital x-ray imaging system for patient positioning at CPO.

S Delacroix, R Ferrand, C Richaud, and E Brune, Centre de Protontherapie d'Orsay, BP 65, Orsay, CEDEX 91402, France

The first treatment room of the CPO, equipped with a PC controlled robotic chair, is mainly dedicated to the treatment of eye and brain tumors.

The ophthalmological throughput has increased to about 200 patients per year, therefore it was necessary to gain time on the daily positioning of patients. Thus, it was decided to install a digital X-ray imaging system.

The main objectives were:

- to reduce the time needed to set up the patient in the treatment position
- to decrease the X-ray dose delivered to the patient.
- to get a dynamic system removable from the optic bench during proton beam irradiation.

We choose two CCD cameras from Medoptics SA, coupled with optic fibres and a fast Lanex Kodak screen. These cameras are connected to a PC and have an independent trigger which allows a simultaneous acquisition of the images.

The software includes different tools:

- measurement of distances and angles
- histograms
- grey profiles along a line
- adjustable zoom for each image displayed

This digital radiography system is very convenient and represents an important economy in time and cost. However, we are keeping the two systems of Polaroid films as backup. The main problem encountered was radiation damage (from neutrons and gamma rays) due to the position of the cameras. We tried to solve this by building a shielded box to protect the axial camera when not in position. As other centres have done, we also tested a 45° mirror to avoid direct X-rays striking the detector. This needs further improvement.

In the near future we would like to develop a second system for the larger fields available in the second treatment room. The aim is to have, through the use of robotic appliances, a total automatisisation of patient set-ups.

\*\*\*\*\*

## An international code of practice for external beam radiotherapy based on absorbed-dose-to-water standards: proton beams.

P. Andreo (IAEA), D. Burns (BIPM), K. Hohlfeld (Germany), M. S. Huq (USA), T. Kanai (Japan), F. Laitano (Italy), V. Smyth (New Zealand) and S. Vynckier (Belgium).

A project has been undertaken during 1997-1999\* to develop an International Code of Practice (CoP) based on standards of absorbed-dose-to-water. It fulfils the need for a systematic and unified approach for dosimetry in radiotherapy with external beams. The final goal is to achieve a coherent dosimetry system, based on the same formalism for practically all radiotherapy beams (except neutrons).

At present, many standards laboratories provide an absorbed-dose-to-water calibration factor of an ionization chamber,  $N_{D,w,Q_0}$ , in a  $^{60}\text{Co}$  reference beam. Some PSDLs also provide such calibrations in high-energy photon and electron beams. The dosimetry of all radiotherapy beams considered in the CoP is based on the  $N_{D,w,Q_0}$  calibration factor of an ionization chamber at a reference beam quality  $Q_0$  together with radiation beam quality correction factors  $k_{Q,Q_0}$ . These correction factors may be calculated. However,

if available, a directly measured value of  $k_{Q,Q_0}$  for the user's chamber in a standards laboratory reference beam is preferred. Values of  $k_{Q,Q_0}$  have been calculated as a function of radiation beam quality for a set of commercially available ionization chambers using a consistent set of physical data (i.e. stopping power ratios, chamber correction factors, etc). These values have been recommended in the CoP.

For proton beams, no primary standard of absorbed dose to water is currently available. However, the dosimetry for these beams can easily be based on the same formalism. Calculated  $k_{Q,Q_0}$  values, with reference to  $^{60}\text{Co}$  gamma-rays ( $Q_0 = ^{60}\text{Co}$ ), are provided for a large number of ionization chambers. They are given as a function of the beam quality specifier  $R_{\text{res}}$  (residual range). Updated values for proton stopping power ratios, which include the effect of nuclear inelastic collisions and secondary electrons, are recommended. A new value for  $(W_{\text{air}})_p$ , based on an objective statistical evaluation of the data available in the literature is used in all calculations. This is consistent with the recommended s-ratios.

The document, presently in draft form and expected to be released during 1999, contains general sections on the formalism and on its implementation, together with a set of different CoPs for each radiation type. Each of these CoPs provides the relevant procedures, data and worksheets for performing user beam calibration. An appendix gives detailed information on the physical parameters used and the estimation of uncertainties.

\*IAEA Co-ordinated Research Project E2.40.09.

The CoP is available at: [http://www.iaea.org/programmes/rihu/e3/dmrp\\_e3\\_codes\\_of\\_prac.html](http://www.iaea.org/programmes/rihu/e3/dmrp_e3_codes_of_prac.html)

\*\*\*\*\*

### **Clinical use of heavy particle dosimetry with ESR (Electron Spin Resonance Spectroscopy).**

F.-J. Prott, U. Haverkamp, C. Wiezorek, and M. Hoffmann, St. Josefs-Hospital, Radiol. Gemeinschaftspraxis, Solmsstr. 15, Wiesbaden, D-65189, Germany.

In radiotherapeutic dosimetry organic solid detectors are commonly used due to their advantage of tissue equivalence, mainly based on the hydrogen abundance.

Hence these dosimetric materials allow application to photons, electrons, protons and neutrons without need of strong corrections for their physical behaviour during absorption as opposed to most of inorganic materials.

The ESR ( Electron Spin Resonance Spectroscopy) meets these demands for independent measurement because the radiation induced radicals are identified and quantified by the unpaired electrons (Zeeman effect). In this study some organic materials (glucose, dextrose, mannose, animal bones) should be irradiated with photons, electrons, protons and light ions in the dose range of 1 to 20 Gy. ESR measurements were made with a commercially available low cost ESR device developed for identification of irradiated foodstuffs.

ESR had the advantage to read the cumulative dose, especially in organic materials, e.g. in bone material. First experience led to a double exposure of the detectors: One irradiation with a known dose (e.g. 10 Gy) of photons (6 MV) to calibrate the individual detector and another irradiation with a measuring dose. The minimum dose, which can be detected is about 0.5 Gy, the accuracy  $\pm 3\%$ . For neutrons (14 MeV) the output for example is 40% lower than for photons (4 to 15 MV).

Success in radiotherapy depends on different fields in medical physics, but these are not independent of each other, the necessary precision in dose delivery demands a close concept. Quality assurance is essential for a safe patient treatment, both dosimetry and treatment planning have to be considered.

\*\*\*\*\*

## **Water Calorimetry and Ionisation Chamber Dosimetry in Collimated Photon, Proton, and Neutron Beams of Various Energies.**

H.J. Brede<sup>1</sup>, K.-D. Greif<sup>1</sup>, O. Hecker<sup>1</sup>, P.J. Binns<sup>2</sup>, K. Langen<sup>2</sup>, D.T.L. Jones<sup>2</sup>, A.N. Schreuder<sup>2</sup>, J. Heese<sup>3</sup> and H. Kluge<sup>3</sup>,  
<sup>1</sup>Physikalisch-Technische Bundesanstalt (PTB), Braunschweig, Germany, <sup>2</sup>National Accelerator Centre (NAC), Faure, South Africa, <sup>3</sup>Hahn-Meitner-Institute (HMI), Berlin, Germany.

A transportable calorimeter has been developed as an absolute device for the determination of the quantity absorbed dose to water with a standard uncertainty of less than 1.5% for a dose rate of greater than 5 mGys<sup>-1</sup>. The compact design and the easy-to-handle operation of the calorimeter make it suitable for use in many different types of clinical beams where either photons, neutrons, protons or heavy ions of differing energies might be used. The calorimeter requires collimated radiation beams with diameters of approximately 40 mm. The temperature increase caused by irradiation is measured with a thermistor probe located at the centre of the calorimeter core. The calorimeter core consists of a cylindrical water-filled gilded aluminium can which is suspended by three thin nylon threads in a vacuum block so as to reduce heat transfer by conduction. In addition, it is operated at a temperature of 4 degrees Celsius to prevent heat transfer in the water by convection. Radiative heat transfer from the core to the surrounding is minimised by using two concentric temperature-controlled shells, where the inner one is maintained at core temperature. The water calorimeter can be used as an absolute standards instrument to determine the absorbed dose to water at the users' facility and ensures the traceability of the calibration of the users' ionisation chambers to a primary standard.

Utilising this water calorimeter and a small ionisation chamber (volume of 0.125 cm<sup>3</sup>) absolute dose measurements were performed in three different types of collimated radiation fields namely a <sup>60</sup>Co photon beam, a neutron beam with a fluence-averaged mean energy of 5.24 MeV, and in two different proton beams with mean energies at the reference measuring position of 36 and 182 MeV respectively. The ionisation chamber was calibrated in the primary standard field of the PTB and the heat defect of water required for the calorimeter in the different charged particles was determined experimentally. The absorbed dose to water inferred from calorimetry was compared to the dose derived from ionometry when applying the radiation field dependent parameters recommended by the neutron and proton protocols of the European Clinical Heavy Particle Dosimetry Group. The mean values of the absolute absorbed dose to water gained with these two independent methods agreed within the standard uncertainty of 1.1% for calorimetry and of 4.5% for ionometry for all types of radiation beams used in this comparison.

\*\*\*\*\*

### **Proton dosimetry intercomparison using parallel plate ion chambers at the PSI-OPTIS proton therapy beam.**

A. Kacperek<sup>2</sup>, E. Egger<sup>1</sup>, A. Amato<sup>3</sup>, L. Barone Tonghi<sup>3</sup>, G. Cuttone<sup>3</sup>, L. Raffaele<sup>3</sup>, A. Rovelli<sup>3</sup>, P. Tabarelli de Fatis<sup>4</sup>, F. Luraschi<sup>4</sup>, and L. Marzoli<sup>4</sup>, <sup>1</sup>Paul Scherrer Institute (CH), <sup>2</sup>Clatterbridge Centre for Oncology (UK), <sup>3</sup>INFN-Laboratori Nazionali del Sud, Catania (I), <sup>4</sup>TERA- Fondazione per adroterapia oncologica (Milano) (I).

A four-centre proton dosimetry intercomparison was performed at the Paul Scherrer Institute on the OPTIS 62 MeV proton beam line. The participating centres were :-

- 1) Paul Scherrer Institute (CH)
- 2) Clatterbridge Centre for Oncology (UK)
- 3) INFN-Laboratori Nazionali del Sud, Catania (I)
- 4) TERA- Fondazione per adroterapia oncologica (Milano) (I)

There were several aims to this study. The first, to intercompare small, parallel-plate ion chambers (IC) in the entrance region of an unmodulated proton beam and the centre-depth of a modulated beam using flat chambers from each centre (MARKUS, graphite windows, 0.055 cm<sup>-3</sup>) in terms of dose-to-water. The second, to obtain a common absorbed dose-to-air calibration, using photons or electrons, and a modification of the formalism proposed by Medin et al<sup>1</sup> such that ,

$$D_w^Q(P_{eff}) = M_Q * N_{D,air,Q_0}^{pp} * [(W_{air})_Q / (W_{air})_{Q_0}] * (S_{\nu}$$

Where Q and Q<sub>0</sub> refer to proton and reference beam qualities, M<sub>q</sub> is the chamber (proton) reading corrected for physical conditions. p<sub>q</sub> refers to perturbation induced by the ion chamber. The physical parameters are drawn from ECHED ('91,'94), ICRU 49 and ICRU draft 6.6. The method of obtaining dose-to-air varied at each centre, using either electrons or <sup>60</sup>Co photon beams and comparing with chambers traceable to international or national standards laboratories<sup>2</sup>. Each centre also used thimble ICs for comparison (T1, Farmer-PTW and FWT-IC18). Provisional results show that the mean of the Markus IC measurements are slightly higher than those obtained from thimble chambers but not significantly so. The deviation of the Markus IC results is small taking into account different calibration and traceability procedures.

Modulated Proton Beam	Maximum Difference %	Average Deviation %	Difference of Means %
MARKUS IC (4)	1.8	0.51	+0.87
Thimble IC (6)	2.7	0.85	-0.6
All IC (10)	3.7	0.97	-----

References: (1) J. Medin, P. Andreo, E. Grussell, O. Mattson, A. Montelius & M. Roos, Phys. Med. Biol. 40 (1995) 1161-76. (2) IAEA Technical Report Series No.277 (1987) and No.381 (1997).

\*\*\*\*\*

### Proton dosimetry in small irradiation fields.

P. van Luijk and J. M. Schippers, Kernfysisch Versneller Instituut, 9747 AA Groningen, the Netherlands.

One of the advantages of proton irradiations is the possibility to reduce the volume of normal tissue exposed to radiation. However, an increase of tumor dose will also increase the dose to normal tissue and new knowledge is necessary to estimate the effects of high doses in small volumes of normal tissue. In the radiobiology program at the KVI we are studying the volume dependence of the tolerance dose of normal tissue. We have used 150 MeV protons from the AGOR cyclotron in Groningen to measure the dose-response curves of the spinal cord of the rat for field sizes ranging from 2 mm to 20 mm. Both homogeneous fields and inhomogeneous fields have been used. In order to compare our results with results previously obtained with photon irradiations, extra attention has been given to the dosimetric aspects of these experiments. The dosimetry for such small irradiation fields is different from dosimetry in large irradiation fields, since standard reference ion chambers require irradiation in a field, which is homogeneous over a sufficiently large volume.

We have used our recently developed dosimetry system, consisting of a scintillating screen, observed with a CCD camera [1], to measure the dose with 0.12 mm/pixel. The relation between light yield and dose has been established by a measurement in a  $\varnothing=80$  mm field, calibrated with a Farmer chamber. To verify the possible influence of a finite position resolution of the CCD+screen system, images of field penumbras (1 mm 20%-80%) were compared to profiles measured with 0.060 mm resolution measurements with a diode. From dose profiles of several field sizes obtained with the same number of monitor units, field-size dependent correction factors (ranging from 1.05 to 1.20) of the monitor have been derived.

[1] S.N. Boon, H. Meertens, P. van Luijk, J.M. Schippers, S. Vynckier, J.M. Denis, J. Medin and E. Grusell, A fast 2D phantom dosimetry system for scanning proton beams, Med. Phys. 25 (1998) 464.

\*\*\*\*\*

### **Experimental study of perturbation correction factors for ionization chambers in a 75 MeV clinical beam.**

H. Palmans, S. Vynckier<sup>1</sup>, J.-M. Denis<sup>1</sup>, F. Verhaegen and H. Thierens, Dept of Biomedical Physics, University of Gent,  
<sup>1</sup>Cliniques universitaires St-Luc, Université Catholique de Louvain, Brussels, Belgium.

Methods for absorbed dose to water determination in clinical proton beams using ionisation chambers have not yet achieved their potential level of accuracy and consistency. Beside the uncertainty on the value of  $(W_{air}/e)_p$  and on the water to air stopping power ratios for protons (or the product of both), there is only little experimental information on chamber dependent perturbation correction factors. They are generally assumed to be unity for proton beams.

In the present work the relative dose to water response of 12 ionisation chambers has been determined in both : the non-modulated and the modulated 75 MeV proton beam at Louvain-la-Neuve. The majority of the ion chambers used in this experiment have a Farmer-type geometry but consist of different combinations of wall materials (graphite, A150, PMMA, nylon) and central electrode materials (aluminium, graphite, A150). All chambers have been calibrated in terms of air kerma as well as in terms of absorbed dose to water in a <sup>60</sup>Co photon beam. Absorbed dose to water in the proton beam could therefore be determined by applying an air kerma based protocol or by applying an absorbed dose to water based formalism using beam quality correction factors  $k_Q$  both obtained using IAEA-data for physical parameters in the <sup>60</sup>Co calibration beam. In both approaches no chamber dependent perturbation correction factors were applied for the proton beam.

A separate experiment with a NE2571-chamber and graphite build-up caps with thicknesses from 1-10 mm was performed in a PMMA phantom in the presence of depth dose gradients. All experimental results are compared with results of Monte Carlo simulations with user codes based on PTRAN and EGS4.

The results for wall perturbation effects in the PMMA phantom show good agreement with calculated results. Based on this knowledge, wall perturbation corrections (up to 0.5% for the set of chambers used) could be derived for the measurements in water in the non-modulated beam.

The measurements in water show that both approaches for absorbed dose to water determination do not give important differences. In general, small but systematic differences between different wall and electrode materials are found. Preliminary results of the electron calculations indicate that the observed experimental differences might be caused by effects from secondary electrons.

\*\*\*\*\*

## **Comparative plans for existing and new proton beamlines at the NAC.**

A.O’Ryan<sup>1</sup>, N. Schreuder<sup>1</sup>, J. Wilson<sup>2</sup>, C. Stannard<sup>2</sup>, F.Vernimmen<sup>3</sup>, R.Abratt<sup>2</sup>, B.Smit<sup>3</sup>, <sup>1</sup>National Accelerator Centre, Cape Town, <sup>2</sup>University of Cape Town, Groote Schuur Hospital, Cape Town, <sup>3</sup>University of Stellenbosch, Tygerberg Hospital, Cape Town

A retrospective study was done on patients with tumours outside the head and neck area that were previously treated at NAC, using the existing horizontal beam facility. Manual laser set-ups were used to position these patients i.e. the Stereophotogrammatic (SPG) system was not used in these cases.

The aim of the study was to ascertain the feasibility of the beam arrangement for the new proton therapy facility currently under construction at NAC. Each plan was carefully investigated with the specific aim to optimize the plan, to minimize the set-up positions (number of beams) and to shorten overall treatment time by using the beam arrangement of the new facility. The new facility will comprise of two fixed beamlines, one at 30° and one at 90° off vertical. This beam arrangement was previously decided on by a workgroup consisting of physicists, clinicians and radiographers. It was also assumed that the patient could be rolled or tilted by a maximum of 15° about the beam lines and rotated through 360 degrees about the vertical axis. An industrial robot arm will be used for patient positioning. The design of the robot allows for a 150 kg payload to be accelerated at very high speeds. By decreasing the acceleration speed, the payload can be increased. The robot has six degrees of freedom and its movements are extremely accurate and reproducible. The each beam line of the new facility will be equipped with a spot scanning beam delivery system. For this study only compensators were used since access to the spot scanning planning system is not yet available.

Results: Fifteen patients were used in this study, with tumours ranging from prostates to adenocarcinoma of the rectum. Out of the 15 plans, 11 could be optimized in various ways. The remaining 4 plans were optimally treated and therefore no gain was achieved. A few cases (plans) will be presented to illustrate the results i.e. 2 prostates , 1 adenocarcinoma rectum and 1 schwannoma. An osteosarcoma case will be presented to illustrate the possible usage of spot scanning.

Conclusion: This study has proved that the new beamlines will be of great benefit to the patients as we constantly strive to improve the dose conformation to the tumour with the patient’s comfort and wellbeing of utmost importance. It also proves that we can achieve the most commonly used angles without the need for a movable gantry.

\*\*\*\*\*

## **Case report on a 12-year-old girl with recurrent benign schwannoma treated with proton therapy.**

D. E. Commin<sup>1</sup>, A. O’Ryan<sup>1</sup>, C. E. Stannard<sup>2</sup>, J. Wilson<sup>2</sup>, F. J. A. Vernimmen<sup>3</sup>, and A. N. Schreuder<sup>1</sup>, <sup>1</sup>National Accelerator Centre, P O box 72, Faure, 7131 South Africa, <sup>2</sup>Groote Schuur Hospital, Observatory, 7925 South Africa, <sup>3</sup>Tygerberg Hospital, Bellville, 7530 South Africa.

Presentation: Presented at the age of 10 years in February 1995 with a large conus and cauda equina tumour with incontinence, paraparesis and pain. The tumour was partially resected, but recurred 2 years later in March 1997. She was referred to the Radiation Oncology Department of the Hillbrow Hospital. Treatment was not given because the planned therapy would cause too many complications. She was then referred to Dr Clare Stannard at Groote Schuur Hospital with a view to particle therapy.

Management: A provisional proton plan was created on a conventional, supine CT scan. Due to the fact that the National Accelerator Centre presently only has a fixed horizontal beam, she was rescanned in 2 oblique positions to achieve this. She was also planned at Tygerberg Hospital on a prone CT scan as the

photon set-up would be easier to achieve. Dose Volume Histograms were then compared. It was proved optimal to treat with protons.

Motivation for treatment: She was an extremely compliant and co-operative young patient with excellent family support. Even though proton therapy was costly, it was the only treatment that would preserve optimal function of the kidneys and small bowel.

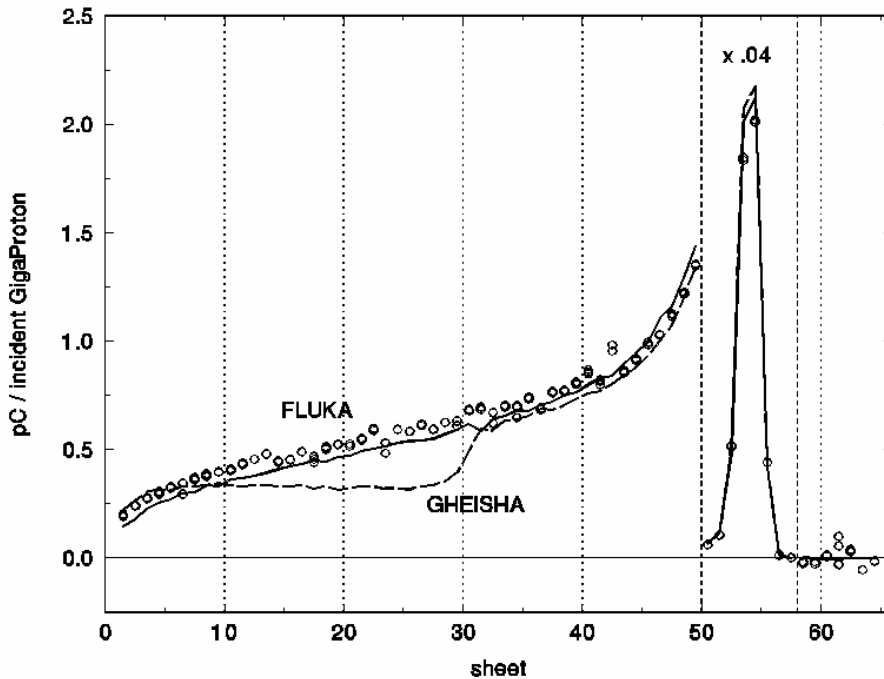
Follow-up: Up to date follow-up will be presented at the congress as the patient will then be 18 months post treatment.

\*\*\*\*\*

**Test of GEANT/FLUKA with 160 MeV protons stopping in copper.**

B. Gottschalk<sup>1</sup>, R. Platais<sup>1</sup>, and H. Paganetti<sup>2</sup>, <sup>1</sup>Harvard Cyclotron Laboratory, 44 Oxford St., Cambridge, MA 02138-1903, USA, <sup>2</sup>Dept. of Radiation Oncology, Massachusetts General Hospital, Boston, MA 02114-2696, USA

We introduce an experimental method to check Monte Carlo nuclear models at proton therapy energies. We have measured the distribution of charge deposited by 160 MeV protons stopping in a stack of insulated copper plates. A buildup region ahead of the main peak contains some 20% of the total charge. It is entirely due to charged secondaries from nuclear interactions, the acceptance for these secondaries is 100%, and we measure charge not dose. Therefore the data provide a good benchmark for nuclear models. We have simulated the stack with GEANT using both FLUKA and the default GHEISHA model. As seen in the figure, FLUKA agrees well but GHEISHA, designed for much higher energies, is unsuitable. (The vertical normalization of experiment and Monte Carlo is absolute, whereas the input energy was increased by .9 MeV above expectations to improve the fit.) The experimental method will work for many other materials including insulators, and measurements in CH<sub>2</sub> are planned.



\*\*\*\*\*

## Implementing the ISO 90001/QART quality system in proton radiotherapy.

A. Kacperek, M. A. Sheen, K. Sztanko, J. Kongerud and B. Marsland, Douglas Cyclotron Unit, Clatterbridge Centre for Oncology, Wirral UK.

The ISO 9001 and 9002 quality systems have been adapted to provide a comprehensive quality system in the radiotherapy environment. This was proposed, in the UK, by the Bleehen Report (1) (1991) following accidents due to among other reasons poor communication and unclear lines on responsibility. More recently, this has been summarised in a report by ESTRO (2). The purpose is to provide a consistent and safe patient treatment and show evidence that this has been done. A quality system is a management system involving document control and internal and external auditing. It is a method of demonstrating agreed procedures have been followed, and supplying a record to this effect. The Quality System does not make assumptions about what is 'best practice', however it is inherent in the system that improvements are identified continually and procedures are rewritten. It may be expressed simply: --

$$\begin{array}{l} \text{(Quality System)} \\ \text{[QART]} \end{array} \times \begin{array}{l} \text{(agreed recommendations)} \\ \text{[local, national etc.]} \end{array} = \text{Quality Assurance}$$

The Clatterbridge Centre for Oncology prepared for registration since 1995, which was obtained in 1998. This included the protontherapy, cyclotron running and radioisotope production.

The introduction of this system was supported at the highest managerial level, from the Chief Executive through the Head of Clinical Radiotherapy. Three types of written documentation are set out in the CCO QART manual:--

LEVEL 1: Requirements of the service, policies, structure, management structure.

LEVEL 2: Written procedures including responsibilities, references.

LEVEL 3: Detailed work instructions ('what to do').

Procedures and work instructions are written in-house by the staff directly involved in the treatment. Internal audits check that procedures have been followed and may suggest improvements. External audits check overall performance of the quality system. Training records indicate which staff are competent to perform specific functions.

Proton therapy at the CCO is unique in the UK although many procedures are adapted from conventional radiotherapy. Best practice in giving protontherapy is governed by cyclotron characteristics e.g. fall-off and beamline design (e.g. penumbra, eye camera), and by performances of existing proton centres. The consistency of proton dosimetry is maintained by international protocols (e.g. ECHED, ICRU) and checked by regular dose intercomparisons. Eyeplanning effectiveness is maintained by peer review at planning meetings and by contact with other centres if the need arises. The integrity of patient data and plans is maintained by strict access rights and training records.

The advantages and disadvantages of the QART system will be discussed as well as specific experiences in proton therapy

References: (1) Quality Assurance in Radiotherapy. Report of a Working Party (*Prof. NM Bleehen*). May 1991. (2) Practical Guidelines for the Implementation of a Quality System in Radiotherapy. ESTRO Quality Assurance Committee. (*J.W.H. Leer et al.*)

\*\*\*\*\*

### **Current status of hadron therapy at the South African National Accelerator Centre.**

D. T. L. Jones<sup>1</sup>, A. N. Schreuder<sup>1</sup>, J. E. Symons<sup>1</sup>, E. A. de Kock<sup>1</sup>, F. J. A. Vernimmen<sup>2</sup>, C. E. Stannard<sup>3</sup>, J. Wilson<sup>3</sup> and J. K. Harris<sup>1</sup>, <sup>1</sup>National Accelerator Centre, P O Box 72, Faure, 7131 South Africa, <sup>2</sup>Tygerberg Hospital, Tygerberg, South Africa, <sup>3</sup>Groote Schuur Hospital, Observatory, South Africa.

The 200 MeV cyclotron facility at the National Accelerator Centre has been operational since 1987. Between September 1988 and December 1998 a total of 992 patients (28938 fields) had been treated on the 66 MeV p + Be isocentric neutron therapy system. The physical beam characteristics are very similar to those of 8 MV x-rays. The facility has operated very reliably with 95% of the scheduled treatments having been successfully completed. Patients are currently being treated according to several protocols, including tumours of the head and neck, salivary gland and breast and soft tissue sarcomas, uterine sarcomas and paranasal sinuses. The installation of a multiblade post-collimator trimmer has improved dose conformation and permits easier and more efficient patient set-up. A prostate treatment programme has recently been implemented. At present neutron therapy is conducted 3 times per week (1 day, 2 nights).

Between September 1993 and December 1998 a total of 291 patients (5378 fields) had been treated (mainly intracranial stereotactic irradiations) on the fixed horizontal 200 MeV proton therapy facility. The facility incorporates an innovative automatic patient positioning system. Of the treatments scheduled 92% have been successfully completed. Conventionally fractionated treatments are also possible as the beam schedule allows for proton treatments on four days per week. Two new fixed beam lines for proton therapy are presently being designed (horizontal and 30° to the vertical) for an existing unused treatment vault. Magnets and other components from a dismantled physics experiment will be utilized. Spot scanning beam delivery and a robotic patient support system will be used. The anticipated completion date of the new facilities is 2001.

\*\*\*\*\*

### **The gamma dose component in a p(66)/Be neutron therapy beam.**

D. T. L. Jones, A. N. Schreuder and J. E. Symons, National Accelerator Centre, P O Box 72, Faure, 7131 South Africa.

In practical situations a neutron fluence is always accompanied by a fluence of gamma rays. These gammas may be generated as part of the neutron production process, or as a result of interactions in the absorbing medium in which the absorbed dose is to be determined, or in the target, collimator, or other irradiated structures. In an extended medium the relative contributions to the absorbed dose from neutrons and from gammas may vary. Although the gamma component in therapy beams is known to be relatively small and the relative biological effect is about 1/3 that of neutrons, it should be determined for accurate dose prescription. Assessment of the gamma component of absorbed dose in a mixed field can be made by the twin-dosimeter method, using a dosimeter which is relatively insensitive to neutrons in conjunction with a tissue-equivalent (TE) ionization chamber. In the present work Geiger-Müller (GM) counters were used as the neutron “insensitive” counters. Their neutron sensitivities are low but have to be measured as they are difficult to calculate. On the other hand the neutron sensitivities of TE ionization chambers are readily calculable.

The neutron sensitivities of two different energy-compensated GM counters were measured in the NAC’s 66 MeV p + Be therapy beam by lead-attenuation methods. In these methods the responses of a

GM counter and a TE ionization chamber in the neutron beam are measured in good geometry as a function of lead absorber thickness. Out-of-beam measurements are also made. From these data the neutron sensitivities of the GM counters can be derived. Both in-beam and out-of-beam measurements were made in phantom under clinical conditions using the twin-dosimeter method. The gamma component on the central axis varies from 3.0% at a depth of 2 cm for a 5.5 x 5.5 cm<sup>2</sup> field to 12.4% at a depth of 40 cm for a 29 x 29 cm<sup>2</sup> field and increases sharply with distance from the edge of the field.

\*\*\*\*\*

### **Pencil beam convolution model for fast dose calculations in uncharged particle radiation treatment planning.**

E. A. de Kock, National Accelerator Centre, P O Box 72, Faure, 7131 South Africa.

An algorithm for the calculation of three-dimensional dose distributions for high-energy photon or neutron beams is presented. The main feature of this algorithm is that the computer calculations are fast enough to allow interactive three-dimensional treatment planning. The algorithm is based on the pencil beam convolution model and shares its features concerning accuracy in complex treatment cases such as irregularly shaped or compensated fields. The speed inherent to the algorithm is achieved by decomposing the pencil beam kernel into a sum of terms in which each term is separated into a product of a depth dependent part and a radial distance dependent part. This decomposition reduces the number of two-dimensional convolutions needed to compute a full three-dimensional dose distribution. The decomposition of the kernel is fully exploited by using the fast Hartley transform to calculate the convolution integrals.

\*\*\*\*\*

### **Energy spectra measured outside the NAC neutron therapy vault.**

V. M. P. Xulubana<sup>1</sup> and P. J. Binns<sup>2</sup>, <sup>1</sup>Physics Dept., University of Western Cape, Cape Town, South Africa, <sup>2</sup>National Accelerator Centre, P O Box 72, Faure, 7131 South Africa

The risks associated with neutron exposures are energy dependent varying by a factor of 4 between intermediate energies and those from either the thermal or fast regions. Consequently characterisation of stray radiation fields around accelerator facilities provides invaluable information for radiation protection purposes.

Low-resolution spectral measurements were performed at the NAC neutron therapy facility using a Bonner multisphere spectrometer (BMS). The spectrometer consists of a 4 x 4 mm LiI(Eu) scintillator that is sensitive to thermal neutrons and a series of six different sized polyethylene moderating spheres. Spectra were measured along the length of the labyrinth leading from the p(66)/Be(40) neutron therapy vault from which the dose equivalents were evaluated. A neutron attenuation of 10<sup>4</sup> is apparent between the entrance and exit to the vault with the thermal contribution measuring from 68 to 89% of the integral flux. Implementation of ICRP60 recommendations increase the dose equivalents by 20 to 50% with the fast neutron component accounting for between 20 and 67% of the measured dose equivalents depending upon position.

\*\*\*\*\*

### **TLD measurements in the hadron therapy beams at NAC.**

J. Bhengu, P. J. Binns, D. T. L. Jones, K. M. Langen, M. Meincken and J. E. Symons, National Accelerator Centre, P O Box 72, Faure, 7131 South Africa.

The use of thermoluminescent dosimeters for *in-vivo* dosimetry in hadron therapy is complicated by a non-linear dose response and the complex nature of the radiation fields. This was investigated for TLD 700 dosimeters in the p(66)Be neutron and 200 MeV proton therapy beams.

Non-linear dose response of the TL-signal was studied over therapeutic dose ranges in both clinical beams. Glow curve analysis enabled the evaluation of separate TL-signals derived from the peak 5 standard dosimetry readout at 200°C and that of peak 6 at 270°C. These results were used to correct the TL-signals for non-linearities in subsequent in-phantom measurements. Depth dose and cross-plane profiles were obtained that compare satisfactorily with standard ionization chamber measurements.

The relative TL-signal of peak 6 to that of 5 varies with LET and could indicate changes in beam quality. The peak 6 to 5 signal ratio corrected for dose dependence was determined as a function of depth and off-axis displacement. Variations qualitatively agree with expected changes in beam quality.

\*\*\*\*\*

### **Correcting microdosimetric spectra for pileup.**

K. Langen<sup>1</sup>, P. Binns<sup>1</sup>, A. Lennox<sup>2</sup>, T. Kroc<sup>2</sup> and P. DeLuca<sup>3</sup>, <sup>1</sup>National Accelerator Centre, Faure, South Africa, <sup>2</sup>Neutron Therapy Facility, Fermilab, Batavia, IL, USA, <sup>3</sup>Department of Medical Physics, University of Wisconsin, Madison, WI, USA.

The acquisition of single event data at the p(66)Be neutron therapy facility (NTF) at Fermilab is complicated by the low duty cycle and high instantaneous dose rate of the beam. Microdosimetric counters are operated in pulse mode and exposure to high instantaneous dose rates causes pulse pileup that may result in spectral distortions. To minimize this problem the instantaneous dose rate was considerably reduced. Spectra measured in this beam however exhibit noticeable discrepancies when compared to those obtained in similar neutron therapy beams which can not be attributed to differences in beam characteristics.

A pileup algorithm was written and applied to an uncorrupted spectrum to test if pileup could produce the observed spectral distortions. A good match between the measured NTF spectrum and that simulated can be achieved by adjusting the degree of pileup. Once the amount of pileup is determined the algorithm is used to correct the corrupted measurement. Correcting the data for pulse pileup enables more reliable integral quantities to be determined from the spectra.

\*\*\*\*\*

### **Dedicated Monte Carlo codes for the NAC proton therapy beam lines.**

A.Tourovsky, A.N. Schreuder, and E.A. de Kock, National Accelerator Centre, PO Box 72, Faure, 7131 South Africa.

A dedicated Monte Carlo (MC) code that is capable to model in full the NAC proton therapy beam line has been recently developed at NAC. The code simulates 3D dose distributions in any 3D object defined as a CT cube. Results of this code have been extensively checked against existing experimental data both for the old and new beam line layouts. The agreement between simulated and measured data for depth

dose curves and lateral profiles was found within 2-3% for all analysed virgin beams (from 1 cm to 10 cm in diameter) and SOBPs (from 5 cm to 8.5 cm) for differently degraded beams ( $R_{50}$  from 8 cm to 16 cm). Monte Carlo simulations also showed that for the NAC beam line the 3D dose results obtained in a water tank are relatively insensitive to fluctuations in the beam initial angular-spatial distribution treated as a product of uncoupled 2D Gaussians. For example, an increase of the initial angular standard deviation by a factor of 30 results in only 5% bend in the central part of the deepest lateral profiles. A multi-field version of the MC code for full verification of treatment plans is currently under development.

\*\*\*\*\*

### **Determination of the energy spectra used for proton therapy at the NAC.**

M. R. Nchodu<sup>1</sup>, F. D. Brooks<sup>2,3</sup>, D. T. L. Jones<sup>3</sup>, A. Buffler<sup>2</sup>, M. S. Allie<sup>2</sup>, P.J. Binns<sup>3</sup>, J. E. Symons<sup>3</sup> and J. V. Siebers<sup>4\*</sup>.

<sup>1</sup>University of the Western Cape, SA, <sup>2</sup>University of Cape Town, SA, <sup>3</sup>National Accelerator Centre, SA, <sup>4</sup>Loma Linda University Medical Centre, USA, \*Present Address: Medical College of Virginia, Virginia Commonwealth University, USA

In order to tailor a proton beam from an accelerator for use in radiotherapy, several beam modification devices have to be introduced between the accelerator and the patient. These devices affect both the dose distribution and the energy spectrum of the beam. Theoretical calculations, e.g. Monte Carlo simulations, can be used to predict the effect of these devices and to obtain the beam characteristics best suited for specific therapy requirements. The reliability of these calculations needs to be checked, however, and this can only be done, ultimately, by experimental measurements.

A detection system has been developed at the NAC [1] to measure the proton spectrum *in situ*, at and close to the isocentre of the patient-treatment position. The proton detection method is based on proton elastic scattering, H(p,p)H, in a thin polyethylene radiator and uses two  $\Delta E-E$  detector telescopes to detect coincident scattered and recoil protons. Spectra have been measured for a variety of proton therapy beams, with and without different beam modification elements, such as beam flatteners, energy degraders and range modulation propellers, in place. The results of these predictions are compared with predictions based on the LAHET Monte Carlo calculations.

\*\*\*\*\*

### **Sacral chordomas treated with neutron and proton therapy.**

S. Schroeder<sup>1</sup>, and J. A. Wilson<sup>2</sup>, <sup>1</sup>National Accelerator Centre, P O Box 72, Faure, 7131 South Africa, <sup>2</sup>Groote Schuur Hospital, Observatory, South Africa

Chordomas are uncommon tumours, locally invasive and they seldom metastasize. They consist of soft gelatinous tissue and can attain a huge size. They are not well controlled by standard doses of EBRT and higher doses and is usually impossible due to nearby critical structures e.g. rectum. Neutrons have been shown to be effective in the treatment of chordomas, but in this anatomical region dose is limited to the tolerance of the rectum. Two case studies are presented, both patients elderly, male presenting with severe pain, sacral swelling and nerve root involvement. Histologically both confirmed as chordoma and inoperable.

A total tumour dose of 16.2 Neutron Gy. was delivered to the primary tumour volume (PTV) in 12 fractions and boosted with a Proton dose of 15 Gy in 6 fractions. NAC is the only facility in the world for both high-energy Neutron and Proton therapy. Mixed modality treatment is particularly useful in radioresistant tumours as the biological advantage of Neutrons can be utilised and in tumours near critical structures where the dose distribution of Protons is essential and therefore offers significant advantages over conventional EBRT in the treatment of sacral chordomas.

\*\*\*\*\*

**Treatment of adenoid cystic carcinoma of the trachea with neutrons.**

J. Waggie, S. Rhoda, C. E. Stannard<sup>2</sup>, <sup>1</sup>National Accelerator Centre, P O Box 72, Faure, 7131 South Africa, <sup>2</sup>Groote Schuur Hospital, Observatory, South Africa.

**CASE STUDY :** Salivary gland tumours are sensitive to neutron therapy; therefore a 63 year old patient with known adenoid cystic carcinoma of the trachea was referred to the N A C for neutron therapy. The tumour had recurred after the patient was treated with palliative photon irradiation one year earlier CT Scan showed a mass and on bronchoscopy the mass was seen to occupy 50% of the circumference of the trachea measuring 4.5 cm in length. The tumour was too large to resect without a high chance of complication or disruption ; thus neutron therapy was indicated. The neutron dose was reduced to 18 gray due to previous radiotherapy and proximity of oesophagus. Symptomatic improvement during treatment occurred and patient has remained asymptomatic for 11 months, although CT Scan at 7 months follow up shows persistent tumour. This demonstrates an encouraging short term response of adenoid cystic carcinoma of trachea to neutron therapy with no early morbidity.

\*\*\*\*\*